Structural Design Optimization of Steel Buildings

Using GS-USA© Frame3D

by

Yogesh Unde

A Thesis Presented in Partial Fulfillment
of the Requirements for the Degree
Master of Science

Approved November 2016 by the
Graduate Supervisory Committee:

Subramaniam Rajan, Chair
Narayanan Neithalath
Barzin Mobasher

ARIZONA STATE UNIVERSITY

December 2016

ABSTRACT

Tall building developments are spreading across the globe at an ever-increasing rate (www.ctbuh.org). In 1982, the number of 'tall buildings' in North America was merely 1,701. This number rose to 26,053, in 2006. The global number of buildings, 200m or more in height, has risen from 286 to 602 in the last decade alone. This dissertation concentrates on design optimization of such, about-to-be modular, structures by implementing AISC 2010 design requirements. Along with a discussion on and classification of lateral load resisting systems, a few design optimization cases are also being studied. The design optimization results of full scale three dimensional buildings subject to multiple design criteria including stress, serviceability and dynamic response are discussed. The tool being used for optimization is GS-USA Frame3D© (henceforth referred to as Frame3D). Types of analyses being verified against a strong baseline of Abaqus 6.11-1, are stress analysis, modal analysis and buckling analysis.

The provisions in AISC 2010 allows us to bypass the *limit state of flexural buckling* in compression checks with a satisfactory buckling analysis. This grants us relief from the long and tedious effective length factor computations. Besides all the AISC design checks, an empirical equation to check beams with high shear and flexure is also being enforced.

In this study, we present the details of a tool that can be useful in design optimization - finite element modeling, translating AISC 2010 design code requirements into components of the FE and design optimization models. A comparative study of designs based on AISC 2010 and fixed allowable stresses, (regardless of the shape of cross section) is also being carried out.

ACKNOWLEDGMENTS

I consider myself very fortunate for the opportunity of working under my advisor, Dr. Subramaniam Rajan. He did not only teach me the work, but he also taught me how to work. I have learnt a lot from his approach towards problem solving and fundamental thinking. This thesis experience has given me invaluable assets. I would like to express my sincere gratitude for his guidance, supervision and encouragement throughout my Masters program. I would also like to extend my gratitude towards Dr. Neithalath and Dr. Mobasher for reviewing my research work.

I dedicate this work to my parents Lata and late Vinod Unde. In addition, I would like to thank my brother Amrut Unde, whom I always look up to, and for supporting me throughout my education.

I would also like to thank Bilal Khaled and Dr. Canio Hoffarth for all the discussions and assistance. I would like to acknowledge all my colleagues at ASU, friends and family for their direct and indirect support.

TABLE OF CONTENTS

Page

CHAPTER Page

LIST OF TABLES

Table Page

LIST OF FIGURES

Figure Page

LIST OF SYMBOLS

A_e	effective net area
A_g	gross c/s area of member
A_w	area of web
C_b	lateral-torsional buckling modification factor
C_w	warping constant
d	overall depth of the section
E	Young's modulus
F_{cr}	critical stress
F_e	elastic buckling stress
f_t	flange thickness
f_w	flange width
F_u	specified minimum tensile strength
F_y	yield stress of steel
G	shear modulus of steel
h	web height less the fillets
h_0	distance between flange centroids
I_x	moment of inertia @ x-axis
I_y	moment of inertia @ y-axis
J	torsional constant
K^1	effective length factor at start node
K^2	effective length factor at end node
K_v	web plate shear buckling coefficient
K_z	length factor for torsional buckling
L	length of the element
M_{cx}	available flexural strength in major axis
M_{cy}	available flexural strength in minor axis
M_{rx}	bending moment in major axis
M_{ry}	bending moment in minor axis
M_{yc}	yield moment in compression flange
N_{max}	maximum axial force
P_c	available axial strength
P_n	allowable axial strength
P_r	required axial strength
Q	net reduction factor for slender elements
Q_a	net reduction factor for web
Q_s	net reduction factor for flange
R_{pc}	web plastification factor
R_{pg}	bending strength reduction factor
r_t	effective radius of gyration for lateral-torsional buckling
r_{xx}	radius of gyration @ x-axis
r_{yy}	radius of gyration @ y-axis
S_x	elastic section modulus @ x-axis
S_{xc}	elastic section modulus referred to compression flange
S_y	elastic section modulus @ y-axis
U	shear lag factor
V_{max}	maximum shear force
V_n	allowable flexural strength
w_h	web height
w_t	web thickness
Z_x	input vector
X_d	plastic section modulus @ x-axis
λ_{pw}	limiting slenderness for a compact web

M_{max}	maximum bending moment	λ_{rw}	limiting slenderness for a non-compact web
M_p	plastic moment capacity		

1 INTRODUCTION

1.1 Brief History

Structural engineering dates back to 2700 B.C. when the step pyramid for Pharaoh Djoser was built by Imhotep, the first engineer in history known by name. Pyramids were the most common major structures built by ancient civilizations because the structural form of a pyramid is inherently stable and can be almost infinitely scaled (as opposed to most other structural forms, which cannot be linearly increased in size, in proportion to increased loads).

Throughout ancient and medieval history most architectural design and construction was carried out by artisans, such as stone masons and carpenters, rising to the role of master builder. No theory of structures existed, and understanding of how structures stood up was extremely limited, and based almost entirely on empirical evidence of 'what had worked before'. Knowledge was retained by guilds and seldom supplanted by advances. Structures were repetitive, and increases in scale were incremental. [1]

Ironically, no record exists of the first calculations of the strength of structural members or the behavior of structural material, but the profession of structural engineer only really took shape with the industrial revolution and the re-invention of concrete. The physical sciences underlying structural engineering began to be understood in the renaissance (period in Europe, from the 14th to 17th century) and have since developed into computer-based applications pioneered in the 1970s. [2]

Dr. Fazlur Rahman Khan was a structural engineer and architect who initiated important structural systems for skyscrapers. ASCE gave him a title of “The father of

tubular designs for high-rises". His innovation was the idea of the 'tube' structural system for tall buildings, including the 'framed tube', 'trussed tube' and 'bundled tube' variations. Most buildings over 40-storeys, constructed since the 1960s, now use a tube design derived from Khan's structural engineering principles. His first building to employ the tube structure was Chestnut De-Witt apartment building in 1963. [3]

Tube structures are very stiff and have numerous significant advantages over other framing systems. They not only make the buildings structurally stronger and more efficient, they significantly reduce the usage of materials while simultaneously allowing buildings to reach even greater heights. The reduction of material makes the buildings economically much more efficient and reduces environmental issues as it results in the least carbon emission impact on the environment. Tubular systems allow greater interior space and further enable buildings to take on various shapes, offering unprecedented freedom to architects. [4]

Following table shows a brief account of past developments in tall buildings. Significance of need to optimize the use of material and carbon footprint is evident from the numbers.

Region	Number of countries	1982		2006	
		Percent	Buildings	Percent	Buildings
North America	4	48.9	1,701	23.9	26,053
Europe	35	21.3	742	23.7	25,809
Asia	35	20.2	702	32.2	35,016
South America	13	5.2	181	16.6	18,129
Africa	41	1.3	47	1	1,078
Total			**3,373**		**106,085**

Table 1.1 Tall buildings in region (reported in Emporis)

1.2 Structural Systems and Classification

In 1969, Fazlur Khan classified structural systems for tall buildings relating to their heights with considerations for efficiency in the form of "Heights for Structural Systems" diagrams. Later, he upgraded these diagrams by way of modifications (Khan, 1972, 1973). He developed these schemes for both steel and concrete.

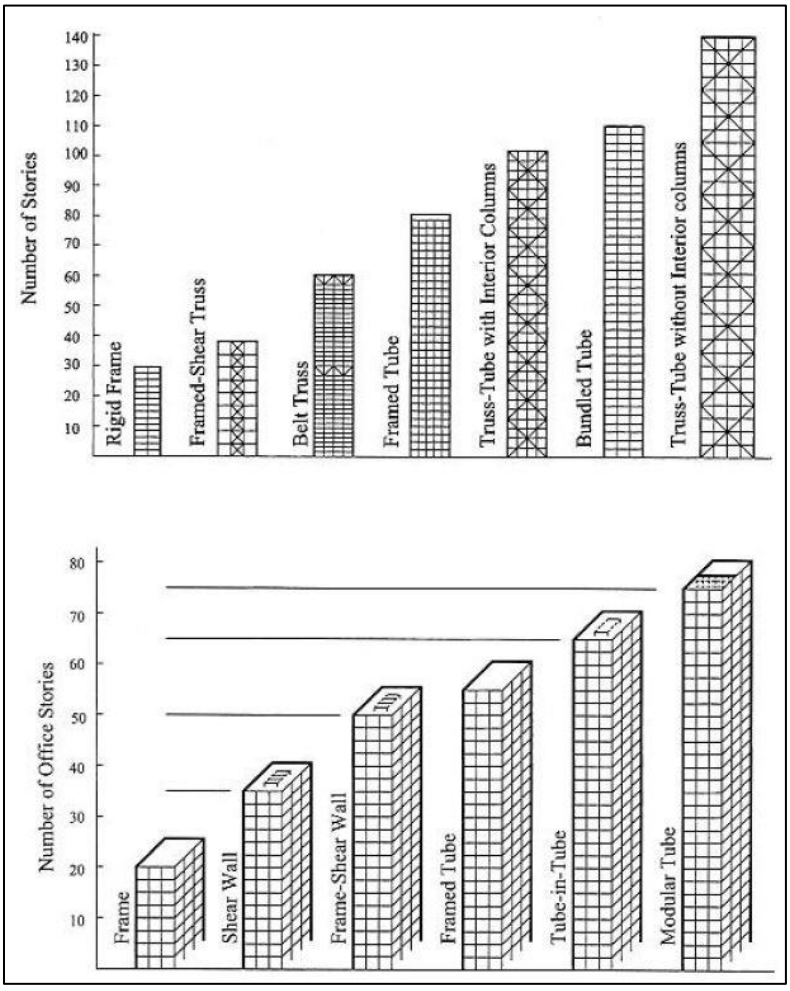

Figure 1.1 Classification of tall buildings by Dr. Falzur Khan

(*above: steel, below: concrete*)

In 2007, Ali and Moon [5] presented a new classification – interior and exterior structures which encompasses most representative tall building structural systems today.

The classification is performed for both primary structures and subsequently auxiliary damping systems. Recognizing the importance of the premium for heights for tall buildings, the classification of structural systems is based on lateral load-resisting capabilities.

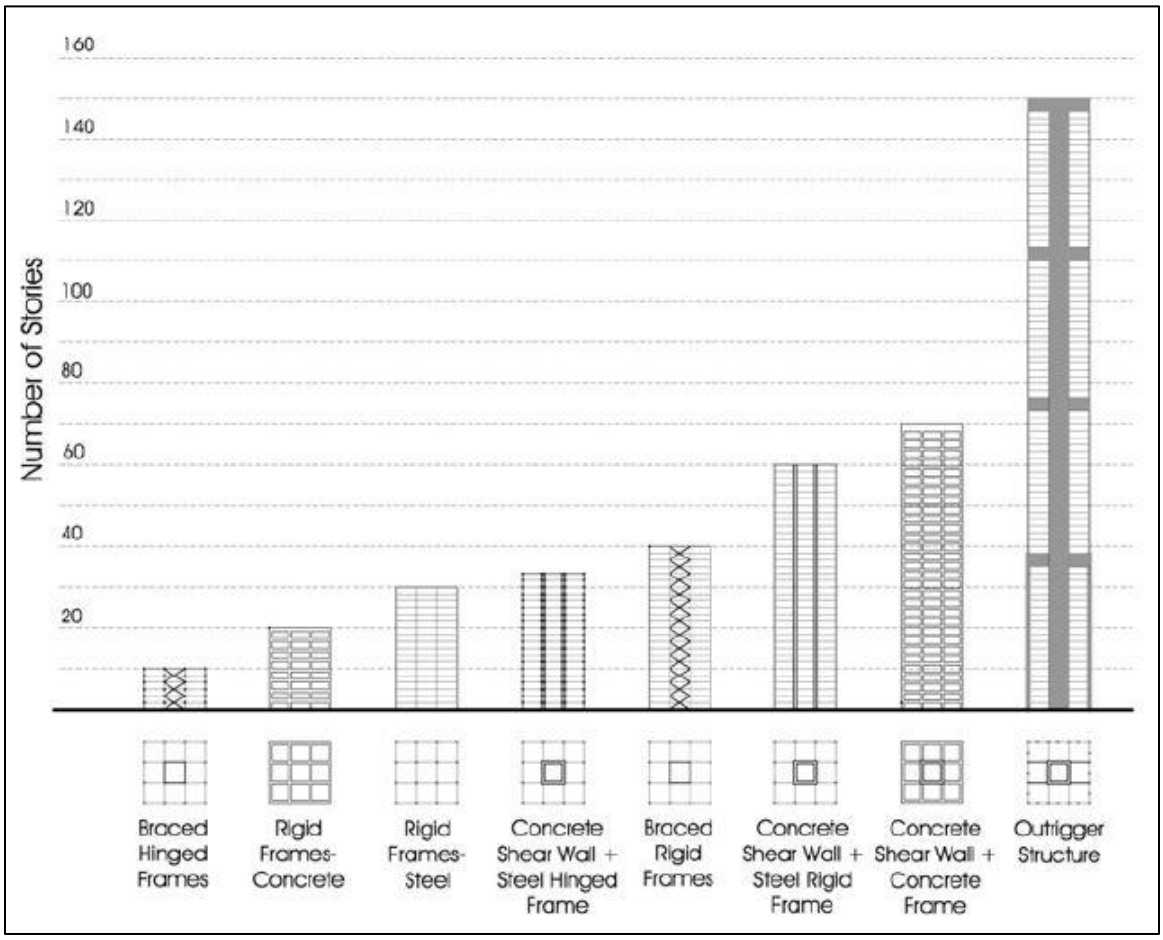

Figure 1.2 Interior Structures classified by Ali and Moon

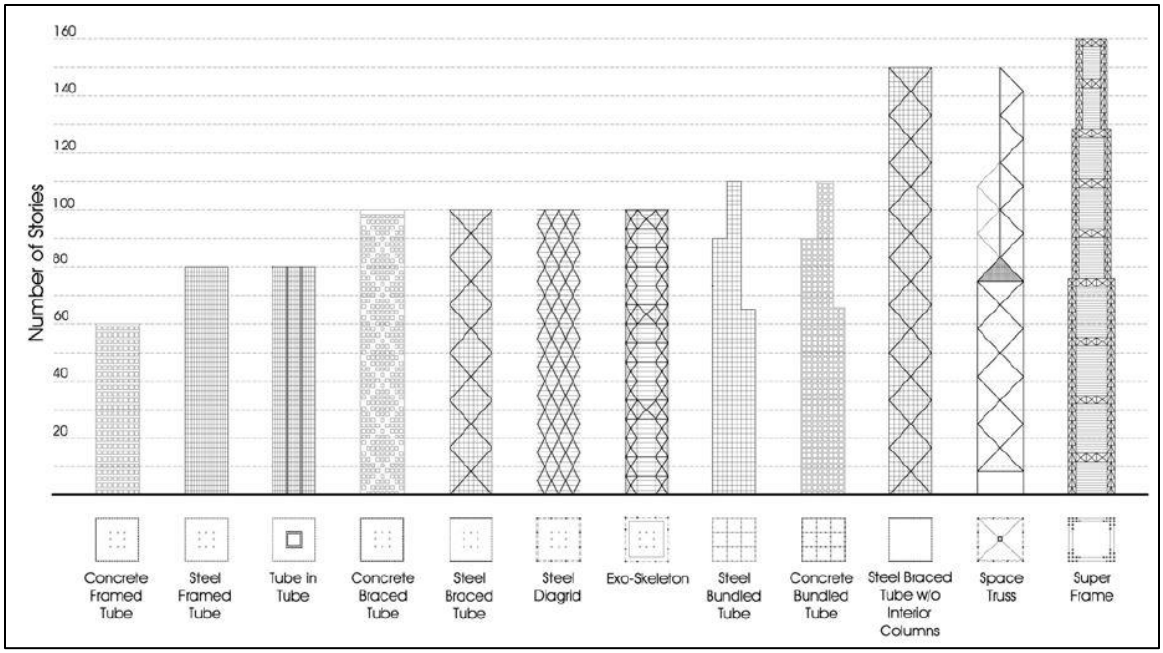

Figure.1.3 Exterior structures classified by Ali and Moon

A detailed categorization, advantages, disadvantages, efficient height limits, etc. is illustrated for both type of structures in tables below (Tables 1.2.1 for interior structures and 1.2.3 for exterior structures).

Category	Sub-Category	Material / Configuration	Efficient Height Limit	Advantages	Disadvantages	Building Examples
Rigid Frames	–	Steel	30	Provide flexibility in floor planning. Fast construction.	Expensive moment connections. Expensive fire proofing.	860 & 880 Lake Shore Drive Apartments (Chicago, USA, 26 stories, 82 m), Business Men's Assurance Tower (Kansas City, USA, 19 stories), Seagram Building, 30th to the top floor (New York, USA, 38 stories, 157 m)
		Concrete	20	Provide flexibility in floor planning. Easily moldable.	Expensive formwork. Slow construction.	Ingalls Building (Cincinnati, USA, 16 stories, 65 m)
Braced Hinged Frames	–	Steel Shear Trusses + Steel Hinged Frames	10	Efficiently resist lateral loads by axial forces in the shear truss members. Allows shallower beams compared with the rigid frames without diagonals.	Interior planning limitations due to diagonals in the shear trusses. Expensive diagonal connections.	Low-rise buildings
Shear Wall / Hinged Frames	–	Concrete Shear Wall + Steel Hinged Frame	35	Effectively resists lateral shear by concrete shear walls.	Interior planning limitations due to shear walls.	77 West Wacker Drive (Chicago, USA, 50 stories, 203.6 m), Casselden Place (Melbourne, Australia, 43 stories, 160 m)
Shear Wall (or Shear Truss) - Frame Interaction System	Braced Rigid Frames	Steel Shear Trusses + Steel Rigid Frames	40	Effectively resists lateral loads by producing shear truss - frame interacting system.	Interior planning limitations due to shear trusses.	Empire State Building (New York, USA, 102 stories, 381 m), Seagram Building, 17th to 29th floor (New York, USA, 38 stories, 157 m)
	Shear Wall / Rigid Frames	Concrete Shear Wall + Steel Rigid Frame	60	Effectively resists lateral loads by producing shear wall - frame interacting system.	Interior planning limitations due to shear walls.	Seagram Building, up to the 17th floor (New York, USA, 38 stories, 157 m)
		Concrete Shear Wall + Concrete Frame	70	"	"	311 South Wacker Drive (Chicago, USA, 75 stories, 284 m), Cook County Administration Building, former Brunswick Building (Chicago, USA, 38 stories, 145 m)
Outrigger Structures	–	Shear Cores (Steel Trusses or Concrete Shear Walls) + Outriggers (Steel Trusses or Concrete Walls) + (Belt Trusses) + Steel or Concrete Composite (Super) Columns	150	Effectively resists bending by exterior columns connected to outriggers extended from the core.	Outrigger structure does not add shear resistance.	Taipei 101 (Taipei, Taiwan, 101 stories, 509 m), Jin Mao Building (Shanghai, China, 88 stories, 421 m)

Table 1.2 Interior structures

Category	Sub Category	Material / Configuration	Efficient Height Limit	Advantages	Disadvantages	Building Examples
Tube	Framed Tube	Steel	80	Efficiently resists lateral loads by locating lateral systems at the building perimeter.	Shear lag hinders true tubular behavior. Narrow column spacing obstructs the view.	Aon Center (Chicago, USA, 83 stories, 346 m)
		Concrete	60	"	"	Water Tower Place (Chicago, USA, 74 stories, 262 m)
	Braced Tube	Steel	100 (With Interior Columns) – 150 (Without Interior Columns)	Efficiently resists lateral shear by axial forces in the diagonal members. Wider column spacing possible compared with framed tubes. Reduced shear lag.	Bracings obstruct the view.	John Hancock Center (Chicago, USA, 100 stories 344 m)
		Concrete	100	"	"	Onterie Center (Chicago, 58 stories, 174 m), 780 Third Avenue (New York, USA, 50 stories, 174 m)
	Bundled Tube	Steel	110	Reduced shear lag.	Interior planning limitations due to the bundled tube configuration.	Sears Tower (Chicago, USA, 108 stories, 442 m)
		Concrete	110	"	"	Carnegie Hall Tower (New York, USA, 62 stories, 230.7 m)
	Tube in Tube	Ext. Framed Tube (Steel or Concrete) + Int. Core Tube (Steel or Concrete)	80	Effectively resists lateral loads by producing interior shear core - exterior framed tube interacting system.	Interior planning limitations due to shear core.	181 West Madison Street (Chicago, USA, 50 stories, 207 m)
Diagrid	–	Steel	100	Efficiently resists lateral shear by axial forces in the diagonal members.	Complicated joints.	Hearst Building (New York, USA, 42 stories, 182 m), 30 St Mary Axe, also known as Swiss Re Building (London, UK, 41 stories, 181 m)
		Concrete	60	"	Expensive formwork. Slow construction.	O-14 Building (Dubai)
Space Truss Structures	–	Steel	150	Efficiently resists lateral shear by axial forces in the space truss members.	Obstruct the view. May obstruct the view.	Bank of China (Hong Kong, China, 72 stories, 367 m)
Superframes	–	Steel	160	Could produce supertall buildings.	Building form depends to a great degree on the structural system.	Chicago World Trade Center (Chicago, USA, 168 stories, Unbuilt)
		Concrete	100	"	"	Parque Central Tower (Caracas, Venezuela, 56 stories, 221 m)
Exo-skeleton	–	Steel	100	Interior floor is never obstructed by perimeter columns.	Thermal expansion / contraction. Systemic thermal bridges.	Hotel de las Artes (Barcelona, Spain, 43 stories, 137 m)

Table 1.3 Exterior structures

1.3 Literature Review

1.3.1 Sizing and Shape Optimization

Due to the complex nature of a modern tall building consisting of thousands of structural members, the traditional trial-and-error design method is generally highly iterative and very time-consuming. Chan *et. al.* [11] presented an automatic resizing technique for the optimal design of tall steel building frameworks. Specifically, a computer-based method was developed for the minimum weight design of lateral load-resisting steel frameworks subject to multiple inter-story drift and member strength and sizing constraints in accordance with building code and fabrication requirements. The most economical standard steel sections to use for the structural members are automatically selected from commercially available standard section databases. The design optimization problem was first formulated and expressed in an explicit form and was then solved by a rigorously derived optimality criteria algorithm. A full-scale 50-story three-dimensional asymmetrical building framework example was presented to illustrate the effectiveness, efficiency, and practicality of the automatic resizing technique. The efficiency of the iterative resizing technique presented, was influenced by the number of constraints and is only weakly dependent on the number of variables. The method provides an effective strategy for the optimal design of tall buildings involving many sizing variables and comparatively fewer drift constraints. An interesting finding is that the optimal design of an asymmetric building framework corresponds to a state in which there is little or almost no building torsion.

1.3.2 Braced Frames

Moon [10] discussed stiffness-based design methodologies for tall building structures with an emphasis on systems with diagonals such as braced tubes and diagrid structures. Guidelines for determination of bending and shear deformations for optimal design, which uses the least amount of structural material to meet the stiffness requirements were presented. The impact of different geometric configurations of the structural members on the material saving economic design is also discussed and recommendations for optimal geometries are made.

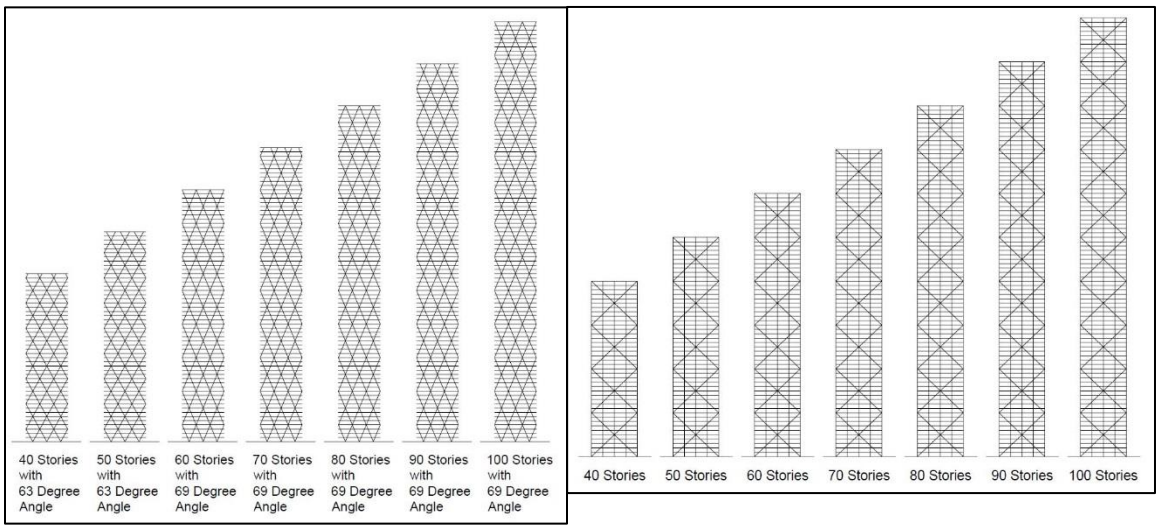

Figure 1.4 Braced tube and Diagrid structures of various heights, aspect ratios and optimal angles (Kyoung Sun Moon, 2008)

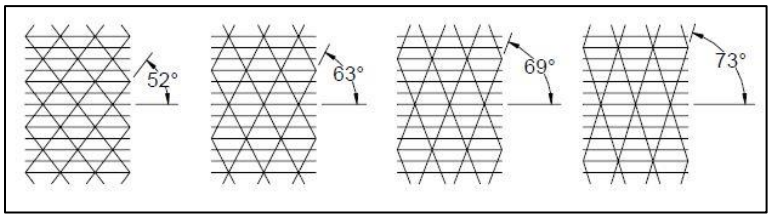

Figure 1.5 Diagrid structures with various diagonal angles

As seen in figures 1.3.2 and 1.3.3, structures of various heights and varying diagrid angles were studied. It was observed that braced framed tube systems performed

best at a diagonal angle nearing 47°. It was also observed with diagrid systems that 63° is near the optimal angle for up to 50 story structures and 69° for structures for and above 60 storeys.

1.3.3 Genetic Algorithm

GA is basically a Direct Search technique, which does not require derivatives. Hence GA has the advantage of being able not only to solve problems where the derivatives are discontinuous but also to find the global minimum. This advantage is offset by an increase in computational requirement – usually the function values are required at a very large number of locations in the design space. The advantage of using GA is that it can handle various types of design variables, including DDV, CDV and Boolean variables. As a result, around 95 percent of structural design optimization work is carried out by implementing GA.

GA is a search strategy based on the rules of natural genetic evolution. Even before the traits of genetic systems were used in solving optimization problems, biologists have used computers to perform simulations of genetic system by the early 1950s. The application of GAs for adaptive systems was first proposed by John Holland (University of Michigan) in 1962.

Because of their discrete nature, GAs lend themselves well to the process of automating the design of skeletal structures. GAs do not require gradient or derivative information. For this reason alone, they have been applied y researchers to solve discrete, non-differentiable, combinatory and global optimization engineering problems, such as transient optimization of gas pipeline, topology design of general elastic mechanical systems, time scheduling, circuit layout design, composite panel design, pipe network

optimization and so on and so forth. GAs are recognized as different from traditional gradient based optimization techniques in the following four major ways [Goldberg, 1989]:

1. GAs work with coding of the design variables and parameters in the problem, rather than the actual parameters themselves.
2. GAs make use of population type search. Many different design points are evaluated during each iteration instead of sequentially moving from one point to the next
3. GAs need only a fitness or objective function value. No derivatives or gradients are necessary.
4. GAs use probabilistic transition rules to find new design points for exploration rather than using deterministic rules based on gradient information to find these new points.

1.3.4 Method of Feasible Directions

The numerical Gradient-based techniques are particularly useful when designing with continuous design variables and continuous and differentiable objective and constraint values. In particular, the Method of Feasible Directions (MFD) [Rajan et al., 2006] is used in this study. Typical problems with about 25-50 design variables can be solved in about 10-15 iterations involving less than a hundred function evaluations and about 10-15 gradient evaluations. The active set strategy is used in order to make the storage space and computations efficient.

Although there are many variations of optimization techniques in existence, the basic structure is that shown in figure 1.3.3.1. [6]

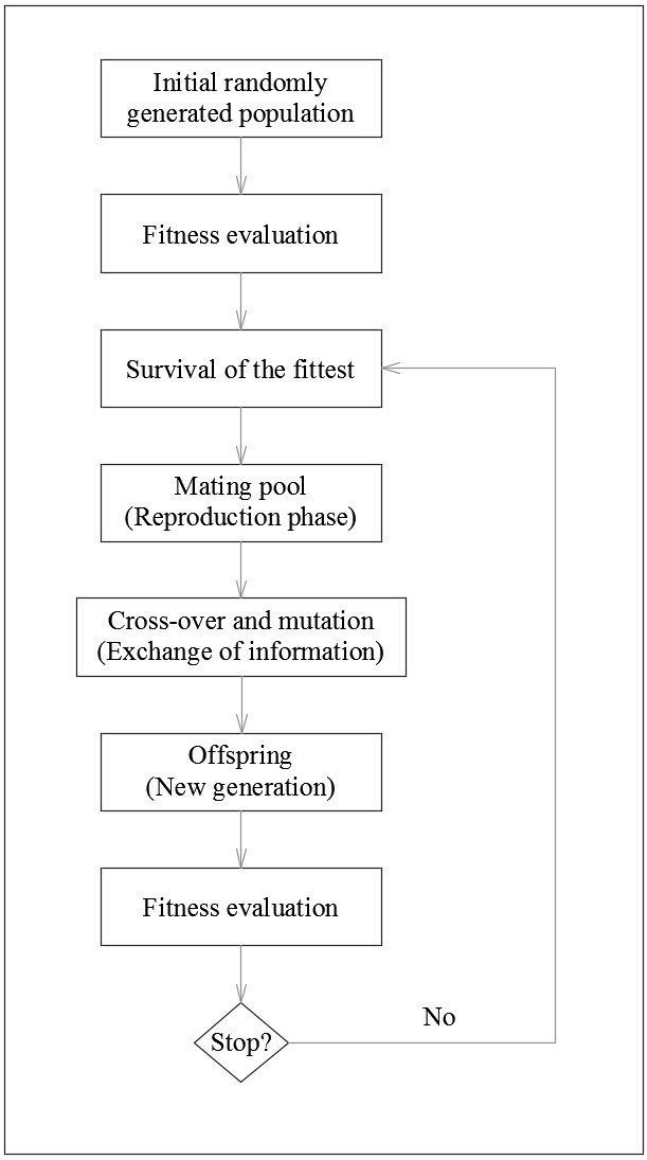

Figure 1.6 Flow in a simple optimization algorithm

1.4 Research Objectives

Most of the structural optimization research is carried out considering the strength based, deflection and drift constraints as design requirements. This work concentrates on structural design optimization of interior and exterior planar frames of ten, twenty, forty and sixty storey buildings. Since it is unconventional to provide bracings in internal frames, the interior frames are necessarily assumed to be ‘rigid’ type structures. For exterior frames, six different types of bracing systems are being designed and optimized for all four buildings. All models are being optimized with AISC 2010 constraints as well as strength based constraints (as separate finite element models) for comparison purposes. Also, lateral deflection, inter-story drift and Euler buckling constraints are being enforced in all models.

An algorithm has been developed from AISC 2010 specifications manual for I-sections and implemented in GS-USA Frame3D program. The structural analysis and design optimization of the building models is accomplished by using the Frame3D program.

2 TYPES OF ANALYSES AND STEEL STRUCTURES

2.1 Finite Element Analysis – Static, Modal and Buckling

The Finite Element Method (FEM) has evolved over a long time. The basic building blocks and ideas originated in the 1940s. With the advancement of technology and computers in 1950s, the ideas were converted into matrix form, making it possible for a practical implementation. [6]

The finite element method is a computer-aided mathematical technique for obtaining approximate numerical solutions to the abstract equations of calculus that predict the response of physical systems subjected to external influences. [7]

Various types of finite element analyses can be applied to pose a single problem, usually a function evaluation, and sometimes to compute constraints. In civil engineering structural analysis, three sets of algebraic equations and/or Eigenvalue problems are solved as follows.

$$\mathbf{K}_{e,d\times d}\mathbf{D}_{d\times lc} = \mathbf{F}_{d\times lc} \tag{2.1.1}$$

$$\mathbf{K}_{e,d\times d}\mathbf{\Phi}_{d\times d} = \mathbf{\Lambda}_{d\times d}\mathbf{M}_{d\times d}\mathbf{\Phi}_{d\times d} \tag{2.1.2}$$

$$\mathbf{K}_{e,d\times d}\mathbf{D}_{d\times lc} = \lambda^{B}\left(-\mathbf{K}_{g,d\times d}\right)\mathbf{D}_{d\times lc} \tag{2.1.3}$$

where $\mathbf{K}_{e,d\times d}$, $\mathbf{M}_{d\times d}$ and $\mathbf{K}_{g,d\times d}$ are the elastic structure stiffness matrix, mass matrix and geometric stiffness matrix respectively. Also, '*d*' is the effective number of degrees-of-freedom in the finite element model, '*lc*' is the number of load cases, 'λ^{B}' is the buckling load factor for the lowest mode. Equations (2.1.2) and (2.1.3) are typically solved in smaller subspaces as $\hat{\mathbf{K}}_{e,q\times q}\mathbf{\Phi}_{q\times q} = \mathbf{\Lambda}_{q\times q}\hat{\mathbf{M}}_{q\times q}\mathbf{\Phi}_{q\times q}$ and

$\hat{\mathbf{K}}_{e,q\times q}\mathbf{D}_{q\times lc} = \lambda^B\left(-\hat{\mathbf{K}}_{g,q\times q}\right)\mathbf{D}_{q\times lc}$, since only the lowest few *'q'* Eigen-pairs are of interest. Detailed explanation on buckling analysis follows.

2.2 Buckling Analysis

The elastic buckling analysis, also known as critical load analysis, is an Eigenvalue problem and is defined as [8]

$$[K_{e,ff}]\{\Delta_f\} = \lambda[-K_{g,ff}]\{\Delta_f\}$$

Where,

$[-K_{g,ff}]$ = 3D Geometric/Stress stiffness matrix, and is calculated from element forces that were obtained from a linear elastic analysis for the applied load configuration $\{P_{ref}\}$.

$[K_{e,ff}]$ = 3D Elastic stiffness matrix.

λ = the Eigenvalue or the ratio of the elastic critical load configuration $\{P_{cr}\}$, to the reference (applied) load configuration $\{P_{ref}\}$.

The geometric stiffness $[-K_{g,ff}]$ is assembled in a way similar to the assembly of elastic stiffness matrix $[K_{e,ff}]$ (using an element matrix in local co-ordinates, transforming the matrix in global co-ordinate system and adding to the corresponding degrees of freedom.).

The 3D Geometric/Stress stiffness matrix for an element in local co-ordinates:

$$[K_g] = \frac{F_{x2}}{L}\begin{bmatrix}
1 & 0 & 0 & 0 & 0 & 0 & -1 & 0 & 0 & 0 & 0 & 0 \\
 & 1.2 & 0 & 0 & 0 & \frac{L}{10} & 0 & -1.2 & 0 & 0 & 0 & \frac{L}{10} \\
 & & 1.2 & 0 & -\frac{L}{10} & 0 & 0 & 0 & -1.2 & 0 & -\frac{L}{10} & 0 \\
 & & & \frac{J}{A} & 0 & 0 & 0 & 0 & 0 & -\frac{J}{A} & 0 & 0 \\
 & & & & \frac{2L^2}{15} & 0 & 0 & 0 & \frac{L}{10} & 0 & \frac{-L^2}{30} & 0 \\
 & & & & & \frac{2L^2}{15} & 0 & -\frac{L}{10} & 0 & 0 & 0 & \frac{-L^2}{30} \\
 & & & & & & 1 & 0 & 0 & 0 & 0 & 0 \\
 & & & & & & & 1.2 & 0 & 0 & 0 & -\frac{L}{10} \\
 & & & & & & & & 1.2 & 0 & \frac{L}{10} & 0 \\
 & & & SYM. & & & & & & \frac{J}{A} & 0 & 0 \\
 & & & & & & & & & & \frac{2L^2}{15} & 0 \\
 & & & & & & & & & & & \frac{2L^2}{15}
\end{bmatrix}$$

Where,

F_{x2} = axial force in the element (negative if compressive and positive if tensile) as a result of linear elastic analysis for the applied loads.

L = Length of the element.

J = Torsional constant.

Jacobi method has been implemented to solve the EVP and obtain the first few Eigenvalues. Therefore, it can be said that, if the first and lowest Eigenvalue is less than

1, i.e. $\frac{\{P_{cr}\}}{\{P_{ref}\}} < 1$, the structure has undergone buckling for the applied load configuration and vice-versa.

2.3 Types of Steel Buildings and Design Codes

This dissertation concentrates on design optimization of planar frames of tall steel buildings, up to sixty storeys. Since it is not a general practice to provide bracing elements (topology optimization) in interior frames of an office building, two different sets of models are being created, namely, *interior* and *exterior* frames. Interior frames are being designed for sizing and shape optimization, whereas exterior frames are being optimized in three areas viz., sizing, shape and topology.

Although, many literatures have established optimum framing systems for exterior structures (figure 1.2.3) as a function of the height, the width is seldom a parameter for optimum designs. For this reason, exterior frames will be optimized topologically using (i) belt trusses, (ii) diagrid systems. and (iii) exo-skeleton types of bracing systems. Regardless of what has been previously established, optimum topology systems will be defined for a particular width and varying heights.

All the steel structures are being designed by implementing AISC 2010 specifications. To carry out a comparative study, all frames designed in accordance with AISC 2010 specifications, are also being designed for strength based constraints (Equation B3-1, AISC 2005). This will also give us confidence in the newly developed technique.

3 AISC 2010 DESIGN CHECKS

3.1 Limit States and Design Requirements

3.1.1 Design of members for tension

1. Slenderness limitations.

   The slenderness ratio L/r preferably should not exceed 300. Where r is minimum of r_{xx} and r_{yy}.

2. Tensile strength.

   The allowable tensile strength, P_n/Ω_t, of tension members shall be the lower value obtained according to the limit states of tensile yielding in the gross section and tensile rupture in the net section.

   1. For tensile yielding in the gross section

      $P_n = F_y A_g$ (D2-1 AISC 2010)

      $\Omega_t = 1.67$ and A_g = gross area of the section

   2. For tensile rupture in the net section

      $P_n = F_u A_e$

      $\Omega_t = 2.0$ and A_e = effective net area = $0.8 A_g U$ (D2-2 AISC 2010)

      Note: Assuming 20% of area for bolt holes.

      U = shear lag factor (maximum of U1 and U2)

      $U1 = 2 f_w f_t / A_g$, (D-3 AISC 2010)

      If $f_w \geq 2/3$ d: $U_2 = 0.9$, else $U_2 = 0.85$ (Table D3.1 Case 7)

3.1.2 Buckling Analysis and Compression Checks

According to Chapter E in AISC 2010 construction manual, the nominal compressive strength, P_n, shall be the lowest value obtained based on the applicable limit states of flexural buckling, torsional buckling and flexural-torsional buckling.

In the case of flexural buckling, the elastic buckling stress is determined according to equation E3-4, as specified in Appendix 7, section 7.2.3(b), or through an elastic buckling analysis, as applicable.

$$F_e = \frac{\pi^2 E}{\left(\frac{KL}{r}\right)^2} \qquad \text{(E3-4 AISC 2010)}$$

This conventional method of arriving at the elastic buckling stress, known as *effective length method*, needs the determination of accurate '*K*' factors by tedious hand procedures and approximate 'charts' provided in the manual. Furthermore, these charts are based on assumptions of idealized conditions, which seldom exist in real structures. These assumptions are as follows:

1. Behavior is purely elastic.
2. All members have constant cross section.
3. All joints are rigid.
4. For columns in frames with sidesway inhibited, rotations at opposite ends of the restraining beams are equal in magnitude and opposite in direction, producing single curvature bending.
5. For columns in frames with sidesway uninhibited, rotations at opposite ends of the restraining beams are equal in magnitude and direction, producing reverse curvature bending.

6. The stiffness parameter $L\sqrt{P/EI}$ of all columns is equal.
7. Joint restraint is distributed to the column above and below the joint in proportion to *EI/L* for the two columns.
8. All columns buckle simultaneously.
9. No significant axial compression force exists in the girders.

Keeping in mind these assumptions, adjustments are often required for

(i) Columns with different end conditions.

(ii) Girders with different end conditions.

(iii) Girders with significant axial loads.

(iv) Column inelasticity.

AISC 2010 does not account for the rotational stiffness provided by non-orthogonal members in a structure. Even after implementing all the above stated conditions in an analysis software, it is very difficult to extract the K values from the 'alignment charts' provided in the manual (*Fig. C-A-7.1 and Fig. C-A-7.2*). In order to avoid these complications and tedious procedures, it is only wise to get the buckling strength of the structure via elastic buckling analysis.

In other words, we can design the structure in such a manner that the lowest Eigenvalue is greater than 1. This implies that the applied loads are not enough for any element in the structure to buckle.

Hence, if the lowest Eigenvalue is greater than 1, it is no longer necessary to check for the limit state of flexural buckling (elastic and/or inelastic buckling) in compression checks. AISC Commentary section 1.3 - 16.1–473 defines the *required axial*

compressive strengths of all members whose flexural stiffness are considered to contribute to lateral stability of the structure, should satisfy the limitation:

$$P_r \leq 0.75P_y$$

Where,

P_r = required axial compressive strength under LRFD or ASD load combinations, kips.

$P_y = F_y A_g$, the axial yield strength, kips.

3.1.3 Modified design procedure

The nominal compressive strength, P_n, shall be the lowest value obtained based on the applicable limit states of flexural buckling, torsional buckling, and flexural-torsional buckling.

The allowable compressive strength = P_n / Ω_c

Where,

$\Omega_c = 1.67$ (Allowable strength design) and

P_n is the nominal compressive strength.

a. Limit state of flexural buckling – for members without slender elements

$$P_n = F_{cr} A_g \qquad \text{(E3-1 AISC 2010)}$$

$$F_{cr} = 0.75F_y$$

b. Limit state of torsional and flexural – torsional buckling – without slender elements

The critical stress F_{cr} shall be determined as follows:

i. When $\frac{F_y}{F_e} \le 2.25$: $F_{cr} = \left[0.658^{\frac{F_y}{F_e}}\right] F_y$ (E7-2 AISC 2010)

ii. When $\frac{F_y}{F_e} > 2.25$: $F_{cr} = 0.877 F_e$ (E7-3 AISC 2010)

Torsional or flexural – torsional buckling stress, F_e, is determined as

$$F_e = \left(\frac{\pi^2 E C_w}{(K_z L)^2} + GJ\right)\frac{1}{I_x + I_y} \quad \text{(E4-4 AISC 2010)}$$

G = Shear modulus of steel

J = Torsional constant

K_z = Effective length factor for torsional buckling

Note: Assuming $K_z = 1.0$ (AISC pg. 16.1-296)

C_w = Warping constant: $C_w = \frac{I_y h_0^{\,2}}{4}$

h_0 = distance between flange centroids

P_n shall be calculated as per section 'a' above.

c. Members with slender elements

The critical stress F_{cr} shall be minimum of:

i. $F_{cr} = 0.75 Q F_y$

ii. When $\frac{QF_y}{F_e} \le 2.25$: $F_{cr} = Q\left[0.658^{\frac{F_y}{F_e}}\right] F_y$ (E7-2 AISC 2010)

iii. When $\frac{QF_y}{F_e} > 2.25$: $F_{cr} = 0.877 F_e$ (E7-3 AISC 2010)

Where,

F_e = elastic buckling stress calculated from E4-4

Q = net reduction factor accounting for all slender compression elements

$= Q_s Q_a$

For sections composed of only slender flange elements, $Q_a = 1$.

For sections composed of only slender web, $Q_s = 1$.

Net reduction factor calculations

1. Slender flange elements, Q_s

   a. When $\frac{f_w}{2f_t} \le 0.56\sqrt{\frac{E}{F_y}}$: $Q_s = 1.0$

   b. When $0.56\sqrt{\frac{E}{F_y}} < \frac{f_w}{2f_t} < 1.03\sqrt{\frac{E}{F_y}}$: $Q_s = 1.415 - 0.74\left(\frac{f_w}{2f_t}\right)\sqrt{\frac{F_y}{E}}$

   c. When $\frac{f_w}{2f_t} \ge 1.03\sqrt{\frac{E}{F_y}}$: $Q_s = \frac{0.69E}{F_y\left(\frac{f_w}{2f_t}\right)^2}$

2. Slender web elements, Q_a

   $$Q_a = \frac{A_e}{A_g}$$

   where,

   A_e = summation of effective areas of the cross section based on the reduced effective width b_e

   b_e is determined as follows

   when $\frac{f_w}{2f_t} \ge 1.49\sqrt{\frac{E}{F_y}}$, $b_e = 1.92 f_t\sqrt{\frac{E}{F_{cr}}}\left[1 - \frac{0.34}{f_w / 2f_t}\sqrt{\frac{E}{F_{cr}}}\right] \le \frac{f_w}{2}$

   with F_{cr} is calculated based on Q = 1.0

3.1.4 Design of members for flexure

The allowable flexural strength = M_n / Ω_b

Where $\Omega_b = 1.67$ (Allowable strength design) and M_n is the nominal flexural strength.

C_b, The lateral-torsional buckling modification factor for non-uniform moment diagrams when both ends of segments are braced is given by:

$$C_b = \frac{12.5M_{max}}{2.5M_{max} + 3M_A + 4M_B + 3M_C} \qquad \text{(F1-1 AISC 2010)}$$

Where,

M_{max} = absolute value of maximum moment in the unbraced segment

M_A = absolute value of moment at quarter point of the unbraced segment

M_B = absolute value of moment at center-line of the unbraced segment

M_C = absolute value of moment at three-quarter point of the unbraced segment

For cantilevers or overhangs, where the free end is unbraced, $C_b = 1.0$

For equal end moments of opposite signs, $C_b = 1.0$

1. Major axis bending
    1. Compact I-shaped members

        M_n shall be lower value obtained according to the limit states of yielding (plastic moment) and lateral-torsional buckling.

        1. Limit state of yielding

            $$M_n = M_p = F_y Z_x \qquad \text{(F2-1 AISC 2010)}$$

            Where,

F_y = specified minimum yield stress of the type of steel being used

Z_x = plastic section modulus about the x-axis.

2. Limit state of lateral-torsional buckling

   1. When $L_b \leq L_p$, the limit state does not apply.

   2. When $L_p < L_b \leq L_r$

$$M_n = C_b\left[M_p - (M_p - 0.7F_yS_x)\left(\frac{L_b - L_p}{L_r - L_p}\right)\right] \leq M_p \qquad \text{(F2-2 AISC 2010)}$$

   3. When $L_b > L_r$, $M_n = F_{cr}S_x \leq M_p$ (F2-3 AISC 2010)

      Where,

      L_b = length between points that are either braced against lateral displacement of the compression flange or braced against twist of the cross section.

$$F_{cr} = \frac{C_b\pi^2 E}{\left(\frac{L_b}{r_{ts}}\right)^2}\sqrt{1 + 0.078\frac{Jc}{S_x h_0}\left(\frac{L_b}{r_{ts}}\right)^2} \qquad \text{(F2-4 AISC 2010)}$$

      Where,

      E = modulus of elasticity of steel,

      J = torsional constant,

      S_x = elastic section modulus taken about the x-axis,

      h_0 = distance between the flange centroids,

      c = 1 for doubly symmetric I-sections.

      The limiting lengths L_p and L_r are determined as follows:

$$L_p = 1.76 r_y \sqrt{\frac{E}{F_y}} \qquad \text{(F2-5 AISC 2010)}$$

$$L_r = 1.95 r_{ts} \frac{E}{0.7F_y} \sqrt{\frac{Jc}{S_x h_0} + \sqrt{\left(\frac{Jc}{S_x h_0}\right)^2 + 6.76\left(\frac{0.7F_y}{E}\right)^2}} \qquad \text{(F2-6 AISC 2010)}$$

Where, $r_{ts}^2 = \frac{\sqrt{I_y C_w}}{S_x}$ (F2-7 AISC 2010)

2. I-shaped members with compact webs and non-compact or slender flanges

   M_n shall be lower value obtained according to the limit states of lateral-torsional buckling and compression flange local buckling.

   1. For limit state of lateral-torsional buckling, same provisions as compact I sections shall apply.
   2. Limit state of compression flange local buckling
      1. For sections with non-compact flanges

$$M_n = M_p - (M_p - 0.7F_y S_x)\left(\frac{\lambda - \lambda_{pf}}{\lambda_{rf} - \lambda_{pf}}\right) \le M_p$$

      2. For sections with slender flanges

$$M_n = \frac{0.9EK_c S_x}{\lambda^2}$$

where,

$\lambda = f_w / 2f_t$,

$\lambda_{pf} = 0.38\sqrt{\frac{E}{F_y}}$ (limiting slenderness for compact flange)

$\lambda_{rf} = \sqrt{\frac{E}{F_y}}$ (limiting slenderness for non-compact flange)

$$0.35 \le K_c = \frac{4}{\sqrt{h / w_t}} \le 0.76$$

where,

h = web height less the fillet radii

3. I-shaped members with non-compact webs

M_n shall be lowest value obtained according to the limit states of compression flange yielding, lateral-torsional buckling and compression flange local buckling.

1. Compression flange yielding

$$M_n = R_{pc} M_{yc} = R_{pc} F_y S_{xc}$$

where,

M_{yc} = yield moment in compression flange

2. Lateral-torsional buckling

1. When $L_b \le L_p$, the limit state of lateral-torsional buckling does not apply.

2. When $L_p < L_b \le L_r$,

$$M_n = C_b \left[R_{pc} M_{yc} - \left(R_{pc} M_{yc} - 0.7 F_y S_{xc} \right) \left(\frac{L_b - L_p}{L_r - L_p} \right) \right] \le R_{pc} M_{yc}$$

3. When $L_b > L_r$, $M_n = F_{cr} S_{xc} \le R_{pc} M_{yc}$

where, $M_{yc} = F_y S_{xc}$

$$F_{cr} = \frac{C_b \pi^2 E}{\left(\frac{L_b}{r_t} \right)^2} \sqrt{1 + 0.078 \frac{J}{S_{xc} h_0} \left(\frac{L_b}{r_t} \right)^2}$$

For $I_{yc} / I_y \leq 0.23$: J = 0

Where,

I_{yc} = moment of inertia of the compression flange about the y-axis

The limiting laterally unbraced length for the limit state of yielding is given by: $L_p = 1.1 r_t \sqrt{\frac{E}{F_y}}$

The limiting unbraced length for the limit state of inelastic lateral-torsional buckling is given by:

$$L_r = 1.95 r_t \frac{E}{0.7F_y} \sqrt{\frac{J}{S_{xc} h_0} + \sqrt{\left(\frac{J}{S_{xc} h_0}\right)^2 + 6.76\left(\frac{0.7F_y}{E}\right)^2}}$$

The web plastification factor, R_{pc} is given by

1. When $I_{yc} / I_y > 0.23$

i. When $\lambda \leq \lambda_{pw}$: $R_{pc} = M_p / M_{yc}$

ii. When $\lambda > \lambda_{pw}$: $R_{pc} = \left[\frac{M_p}{M_{yc}} - \left(\frac{M_p}{M_{yc}} - 1\right)\left(\frac{\lambda - \lambda_{pw}}{\lambda_{rw} - \lambda_{pw}}\right)\right] \leq \frac{M_p}{M_{yc}}$

2. When $I_{yc} / I_y \leq 0.23$: $R_{pc} = 1.0$

Where,

$M_p = F_y Z_x \leq 1.6 F_y S_{xc}$

S_{xc} = elastic section modulus referred to compression flange (AISC 2010 pg. 16.1-311)

$\lambda = \frac{h_c}{W_t}$

λ_{pw} = the limiting slenderness for a compact web

λ_{rw} = the limiting slenderness for a non-compact web

h_c = twice the distance from the centroid to the inside face of the compression flange less the fillet or corner radius.

The effective radius of gyration for lateral-torsional buckling, r_t, is given by $r_t = \frac{f_w}{\sqrt{12\left(\frac{h_0}{d} + \frac{a_w W_h^{\,2}}{6h_0 d}\right)}}$, where $a_w = \frac{h_c W_t}{f_w f_t}$

3. Compression flange local buckling

    1. For sections with compact flanges, the limit state of local buckling does not apply.
    2. Sections with non-compact flanges,

$$M_n = R_{pc}M_{yc} - \left(R_{pc}M_{yc} - 0.7F_y S_{xc}\right)\left(\frac{\lambda - \lambda_{pf}}{\lambda_{rf} - \lambda_{pf}}\right)$$

    3. For sections with slender flanges,

$$M_n = \frac{0.9Ek_c S_{xc}}{\lambda^2}$$

    where all parameters are as defined earlier.

4. I-shaped members with slender webs

    M_n shall be lowest value obtained according to the limit states of compression flange yielding, lateral-torsional buckling and compression flange local buckling.

1. Compression flange yielding

$$M_n = R_{pg} F_y S_{xc}$$

2. Lateral torsional buckling

$M_n = R_{pg} F_{cr} S_{xc}$

1. When $L_b \le L_p$, the limit state of lateral-torsional buckling does not apply.

2. When $L_p < L_b \le L_r$, $F_{cr} = C_b \left(F_y - (0.3F_y)\left(\frac{L_b - L_p}{L_r - L_p} \right) \right) \le F_y$

3. When $L_b > L_r$, $F_{cr} = \frac{C_b \pi^2 E}{\left(\frac{L_b}{r_t} \right)^2} \le F_y$

Where,

$$L_p = 1.1 r_t \sqrt{\frac{E}{F_y}},$$

$$L_r = \pi r_t \sqrt{\frac{E}{0.7F_y}},$$

R_{pg} = bending strength reduction factor:

$$R_{pg} = 1 - \frac{a_w}{1200 + 300a_w}\left(\frac{h_c}{W_t} - 5.7\sqrt{\frac{E}{F_y}} \right) \le 1.0,$$

$$a_w = \frac{h_c W_t}{f_w f_t} \le 10,$$

$$r_t = \frac{f_w}{\sqrt{12\left(\frac{h_0}{d} + \frac{a_w W_h^{\,2}}{6h_0 d} \right)}}$$

3. Compression flange local buckling

$M_n = R_{pg} F_{cr} S_{xc}$

1. For sections with compact flanges, the limit state of compression flange local buckling does not apply.
2. For sections with non-compact flanges

$$F_{cr} = F_y - (0.3F_y)\left(\frac{\lambda - \lambda_{pf}}{\lambda_{rf} - \lambda_{pf}}\right)$$

3. For sections with slender flanges

$$F_{cr} = \frac{0.9Ek_c}{\lambda^2}$$

Where,

$$0.35 \le K_c = \frac{4}{\sqrt{h / w_t}} \le 0.76,$$

$$\lambda = \frac{f_w}{2 f_t}$$

2. Minor axis bending

   M_n shall be lower value obtained according to the limit states of yielding (plastic moment) and flange local buckling.

   1. Yielding

      $$M_n = M_p = F_y Z_y \leq 1.6\, F_y S_y$$

   2. Flange local buckling

      1. For sections with compact flanges, the limit state of flange local buckling does not apply.

      2. For sections with non-compact flanges

         $$M_n = M_p - (M_p - 0.7 F_y S_y)\left(\frac{\lambda - \lambda_{pf}}{\lambda_{rf} - \lambda_{pf}}\right)$$

      3. For sections with slender flanges

         $$M_n = F_{cr} S_y$$

         Where,

         $$F_{cr} = \frac{0.69E}{\lambda^2}$$

         $\lambda = f_w / 2f_t$

         S_y = elastic section modulus taken about the y-axis.

3.1.5 Design of members for shear

The allowable flexural strength = V_n / Ω_v

Where $\Omega_v = 1.67$ (Allowable strength design)

and V_n is the nominal shear strength.

1. Shear strength – major axis

The nominal shear strength V_n, of unstiffened or stiffened webs according to the limit state of shear yielding and shear buckling is

$$V_n = 0.6 F_y A_w C_v \qquad \text{(G2-1 AISC 2010)}$$

Where,

A_w = area of web, overall depth times the web thickness, $d\ w_t$,

h = the clear distance between flanges less the fillet or corner radii,

w_t = thickness of web.

For C_v,

a. If $\frac{h}{w_t} \le 2.24\sqrt{\frac{E}{F_y}}$, $\Omega_v = 1.50$ and $C_v = 1.0$.

b. Else,

i. When $\frac{h}{w_t} \le 1.10\sqrt{K_v \frac{E}{F_y}}$, $C_v = 1.0$

ii. When $1.10\sqrt{K_v \frac{E}{F_y}} < \frac{h}{w_t} \le 1.37\sqrt{K_v \frac{E}{F_y}}$,

$$C_v = \frac{1.10\sqrt{K_v \frac{E}{F_y}}}{\frac{h}{w_t}} \qquad \text{(G2-4 AISC 2010)}$$

iii. When $\frac{h}{w_t} > 1.37\sqrt{K_v \frac{E}{F_y}}$, $C_v = \frac{1.51 K_v E}{\left(\frac{h}{w_t}\right)^2 F_y}$ (G2-5 AISC 2010)

The web plate shear buckling coefficient, K_v, for webs without transverse stiffeners and with $\frac{h}{w_t} < 260$, $K_v = 5$.

2. Shear strength – minor axis (G7 AISC 2010)

For doubly symmetric shapes loaded in the weak axis without torsion, the nominal shear strength, V_n, for each shear resisting element shall be determined using equation G2-1 and section G2-1(b) with $A_w = 2b_f t_f, h/t_w = b/t_f, k_v = 1.2$, and b = half of the full-flange width, b_f in. (mm).

Note: For all ASTM A6 W shapes, when $F_y \leq 50$ ksi (345 MPa), $C_v = 1.0$

3.1.6 Design of members for combined effects

1. Members subjected to flexure and compression.

   The interaction of flexure and compression shall be limited by:

   a. When $\frac{P_r}{P_c} \geq 0.2$, $\frac{P_r}{P_c} + \frac{8}{9}\left(\frac{M_{rx}}{M_{cx}} + \frac{M_{ry}}{M_{cy}}\right) \leq 1.0$ (H1-1a AISC 2010)

   b. When $\frac{P_r}{P_c} < 0.2$, $\frac{P_r}{2P_c} + \frac{8}{9}\left(\frac{M_{rx}}{M_{cx}} + \frac{M_{ry}}{M_{cy}}\right) \leq 1.0$ (H1-1b AISC 2010)

   Where,

   P_r = Required axial strength using ASD load combinations,

   P_c = Available axial strength = P_n / Ω_c,

   M_r = Required flexural strength,

   M_c = Available flexural strength = M_n / Ω_b,

   x: Subscript relating symbol to strong axis bending and shear,

   y: Subscript relating symbol to weak axis bending and shear.

2. Members subjected to flexure and tension

   The interaction of tension and flexure, constrained to bend about a geometric axis (x and/or y) shall be limited by equations H1-1a and H1-1b.

   Where,

   P_c = Available axial strength, = P_n / Ω_t

   Allowable tensile strength P_n / Ω_t shall be the lower value obtained according to the limit states of tensile yielding in the gross section and tensile rupture in the net section.

1. For tensile yielding in the gross section

   $P_n = F_y A_g$ and $\Omega_t = 1.67$

2. For tensile rupture in the net section

   $P_n = F_u A_e$ and $\Omega_t = 2.00$

   Where,

   A_e = effective net area,

   A_g = gross area of the member,

   F_y = specified minimum yield stress,

   F_u = specified minimum tensile strength.

   C_b in equation F1-1 may be multiplied by $\sqrt{1+\frac{\alpha P_r}{P_{ey}}}$ for axial tension that acts concurrently with flexure. Where $P_{ey} = \frac{\pi^2 E I_y}{L_b^{\,2}}$ and $\alpha = 1.6$

3. Members subjected to high flexure and high shear

   When a beam element is subjected to relatively large shear and bending moment at the same location, the beam cannot provide its full capacity either in shear or in moment. As a result, an empirical interaction equation is used to check the adequacy of the beam. V_c = Available shear strength = V_n / Ω

   If $0.6V_c \le V_u \le V_c$, and if $0.75M_c \le M_u \le M_c$ with $\Omega = 1.67$, beams must satisfy the following interaction equations. [9]

   1. $\frac{M_{ux}}{M_{cx}} + 0.625\frac{V_{ux}}{V_{cx}} \le 1.375$

   2. $\frac{M_{uy}}{M_{cy}} + 0.625\frac{V_{uy}}{V_{cy}} \le 1.375$

3.2 Implemented algorithms

3.2.1a Design checks for tensile force

1. Get the length, r_{xx} and r_{yy} of the member;

   r = minimum of r_{xx} and r_{yy}

2. If $L/r < 300$: check (1) = OK,

   else: check (1) = slender element.

3. Get the axial force P_a, F_y and A_g of the member.

4. Tensile strength in yielding: $P_{n1} = F_y A_g / 1.67$

5. Get the element properties vector $\mathbf{X_d}$

6. Total depth of section, $d = w_h + 2\ f_t$

7. Shear lag factor:

   $U_1 = 2\ f_w\ f_t / A_g$

   If $f_w \geq 2/3\ d$: $U_2 = 0.85$,

   else $U_2 = 0.9$

8. U = maximum of U_1 and U_2

9. Effective net area $A_e = 0.8 A_g\ U$ (Assuming 20% bolt holes)

10. Tensile strength in rupture: $P_{n2} = 0.5 F_u A_e$

11. P_n = minimum of P_{n1} and P_{n2}

12. Return P_a / P_n:

3.2.1b Design checks for compressive force

1. Classify the flange

   a. If $\frac{f_w}{2f_t} < 0.56\sqrt{\frac{E}{F_y}}$: section has non-slender flanges (fl = NS)

   b. else: section has slender flanges (fl = S)

2. Classify the web

   a. If $\frac{h}{w_t} < 1.49\sqrt{\frac{E}{F_y}}$: section has non-slender web (web = NS, Q_a = 1.0)

   b. else: section has slender web (web = S)

3. If fl = NS and web = NS

   a. Calculate F_{cr1} (limit state of flexural buckling):

      $F_{cr1} = 0.75F_y$

   b. Calculate F_{cr2} (limit state of flexural-torsional buckling):

      i. $h_0 = W_h + f_t$, $C_w = \frac{I_y h_0^2}{4}$, $F_{e2} = \left(\frac{\pi^2 EC_w}{(K_z L)^2} + GJ\right)\frac{1}{I_x + I_y}$

      ii. If $\frac{F_y}{F_{e2}} \le 2.25$: $F_{cr2} = \left[0.658^{\frac{F_y}{F_{e2}}}\right]F_y$,

      else: $F_{cr2} = 0.877F_{e2}$

   c. F_{cr} = minimum of F_{cr1} and F_{cr2}.

   d. $P_n = F_{cr}A_g / 1.67$

4. If fl = S or web = S

   Net reduction factor calculations:

   a. If fl = NS: Q_s = 1.0

b. If $0.56\sqrt{\frac{E}{F_y}} < \frac{f_w}{2f_t} < 1.03\sqrt{\frac{E}{F_y}}$: $Q_s = 1.415 - 0.74\left(\frac{f_w}{2f_t}\right)\sqrt{\frac{F_y}{E}}$

c. else if $\frac{f_w}{2f_t} \geq 1.03\sqrt{\frac{E}{F_y}}$: $Q_s = \frac{0.69E}{F_y\left(\frac{f_w}{2f_t}\right)^2}$

d. If $\frac{f_w}{2f_t} \geq 1.49\sqrt{\frac{E}{F_y}}$:

i. $F_{cr1} = 0.75F_y$

ii. $h_0 = W_h + f_t$, $C_w = \frac{I_y h_0^{\,2}}{4}$, $F_{e2} = \left(\frac{\pi^2 EC_w}{(K_z L)^2} + GJ\right)\frac{1}{I_x + I_y}$

iii. If $\frac{F_y}{F_{e2}} \leq 2.25$: $F_{cr2} = \left[0.658^{\frac{F_y}{F_{e2}}}\right]F_y$,

else: $F_{cr2} = 0.877F_{e2}$

e. F_{cr} = minimum of F_{cr1} and F_{cr2}.

f. $b_e = 1.92f_t\sqrt{\frac{E}{F_{cr}}}\left[1 - \frac{0.34}{f_w / 2f_t}\sqrt{\frac{E}{F_{cr}}}\right] \leq b$, $A_e = (W_h W_t) + (4b_e f_t)$

g. $Q_a = \frac{A_e}{A_g}$, $Q = Q_s Q_a$

h. check:

i. $F_{cr1} = 0.75QF_y$

ii. $h_0 = W_h + f_t$, $C_w = \frac{I_y h_0^{\,2}}{4}$, $F_{e2} = \left(\frac{\pi^2 EC_w}{(K_z L)^2} + GJ\right)\frac{1}{I_x + I_y}$

iii. If $\frac{F_y}{F_{e2}} \le 2.25$: $F_{cr2} = Q\left[0.658^{\frac{F_y}{F_{e2}}}\right]F_y$,

else: $F_{cr2} = 0.877F_{e2}$

i. F_{cr} = minimum of F_{cr1} and F_{cr2}.

j. $P_n = F_{cr}A_g / 1.67$

k. P_n = minimum of $P_n(3)$, $P_n(4)$

5. Return P_a / P_n:

3.2.2a Design checks for shear force (major axis)

1. If $\frac{h}{w_t} \le 2.24\sqrt{\frac{E}{F_y}}$: $\Omega_v = 1.50$ and $C_v = 1.0$,

   else: $\Omega_v = 1.67$

2. $K_v = 5.0$

3. If $\frac{h}{w_t} \le 1.10\sqrt{K_v \frac{E}{F_y}}$: $C_v = 1.0$

4. Else if $1.10\sqrt{K_v \frac{E}{F_y}} < \frac{h}{w_t} \le 1.37\sqrt{K_v \frac{E}{F_y}}$: $C_v = \frac{1.10\sqrt{K_v \frac{E}{F_y}}}{\frac{h}{w_t}}$

5. Else if $\frac{h}{w_t} > 1.37\sqrt{K_v \frac{E}{F_y}}$: $C_v = \frac{1.51 K_v E}{\left(\frac{h}{w_t}\right)^2 F_y}$

6. $V_n = 0.6\, F_y\, A_w\, C_v / \Omega_v$

7. Return (V_a / V_n)

3.2.2b Design checks for shear force (minor axis)

1. If $\frac{f_w}{2f_t} \le 2.24\sqrt{\frac{E}{F_y}}$: $\Omega_v = 1.50$ and $C_v = 1.0$,

   else: $\Omega_v = 1.67$

2. $K_v = 1.2$, $A_w = 2 f_w f_t$

3. If $\frac{f_w}{2f_t} \le 1.10\sqrt{K_v \frac{E}{F_y}}$: $C_v = 1.0$

4. Else if $1.10\sqrt{K_v \frac{E}{F_y}} < \frac{f_w}{2f_t} \le 1.37\sqrt{K_v \frac{E}{F_y}}$: $C_v = \frac{1.10\sqrt{K_v \frac{E}{F_y}}}{\frac{f_w}{2f_t}}$

5. Else if $\frac{f_w}{2f_t} > 1.37\sqrt{K_v \frac{E}{F_y}}$: $C_v = \frac{1.51 K_v E}{\left(\frac{f_w}{2f_t}\right)^2 F_y}$

6. $V_n = 0.6\, F_y\, A_w\, C_v / \Omega_v$

7. Return (V_a / V_n)

3.2.3a Design checks for flexure (major axis)

1. Classify the flange

   a. If $\frac{f_w}{2f_t} < 0.38\sqrt{\frac{E}{F_y}}$: section has compact flanges (fl = C)

   b. If $0.38\sqrt{\frac{E}{F_y}} < \frac{f_w}{2f_t} < \sqrt{\frac{E}{F_y}}$: section has non-compact flanges (fl = NC)

   c. If $\frac{f_w}{2f_t} > \sqrt{\frac{E}{F_y}}$: section has slender flanges (fl = S)

2. Classify the web

   a. If $\frac{h}{w_t} < 3.76\sqrt{\frac{E}{F_y}}$: section has compact web (web = C)

   b. If $3.76\sqrt{\frac{E}{F_y}} < \frac{h}{w_t} < 5.7\sqrt{\frac{E}{F_y}}$: section has non-compact web (web = NC)

   c. If $\frac{h}{w_t} > 5.7\sqrt{\frac{E}{F_y}}$: section has slender web (web = S)

3. If check is being carried out for flexure and tension:

$$C_b = \sqrt{1+\frac{1.6P_rL_b^2}{\pi^2 EI_y}}\left(\frac{12.5M_{\max}}{2.5M_{\max}+3M_A+4M_B+3M_C}\right)$$

   else: $$C_b = \frac{12.5M_{\max}}{2.5M_{\max}+3M_A+4M_B+3M_C}$$

4. If section is compact (web = C and fl = C):

   a. Yielding: $M_{n1} = M_p = F_y Z_x$

   b. L-T buckling: $L_p = 1.76r_y\sqrt{\frac{E}{F_y}}$, $L_b = L$, $h_0 = W_h + f_t$

i. If $L_b < L_p$: $M_{n2} = M_{n1}$

ii. $r_{ts}^{\ 2} = \frac{\sqrt{I_y C_w}}{S_x}$, $L_r = 1.95 r_{ts} \frac{E}{0.7F_y} \sqrt{\frac{J}{S_x h_0} + \sqrt{\left(\frac{J}{S_x h_0}\right)^2 + 6.76\left(\frac{0.7F_y}{E}\right)^2}}$

iii. If $L_p < L_b \le L_r$: $M_{n2} = C_b \left[M_p - (M_p - 0.7F_y S_x)\left(\frac{L_b - L_p}{L_r - L_p}\right)\right] \le M_p$

iv. If $L_b > L_r$: $F_{cr} = \frac{C_b \pi^2 E}{\left(\frac{L_b}{r_{ts}}\right)^2} \sqrt{1 + 0.078 \frac{J}{S_x h_0}\left(\frac{L_b}{r_{ts}}\right)^2}$,

$M_{n2} = F_{cr} S_x$

c. M_n = minimum of M_{n1} and M_{n2}

5. If fl = NC or fl = S and web = C

a. For lateral torsional buckling, obtain M_{n1} from 4.b

b. Compression flange local buckling:

i. $\lambda = f_w / 2f_t$, $\lambda_{pf} = 0.38\sqrt{\frac{E}{F_y}}$, $\lambda_{rf} = \sqrt{\frac{E}{F_y}}$

ii. If fl = NC: $M_{n2} = M_p - (M_p - 0.7F_y S_x)\left(\frac{\lambda - \lambda_{pf}}{\lambda_{rf} - \lambda_{pf}}\right) \le M_p$

iii. If fl = S: $0.35 \le K_c = \frac{4}{\sqrt{h / w_t}} \le 0.76$, $M_{n2} = \frac{0.9EK_c S_x}{\lambda^2}$

c. M_n = minimum of M_{n1} and M_{n2}

6. If web = NC

a. I_{yc} = Moment of inertia of the compression flange @ y-axis = $f_t\ f_w^3 / 12$

b. $h_c = h$, $S_{xc} = S_{xt} = I_x / (W_h/2 + f_t)$

c. $M_p = F_y Z_x \le 1.6\, F_y S_{xc}$, $M_{yc} = F_y S_{xc}$, $\lambda_{pw} = 3.76\sqrt{\frac{E}{F_y}}$, $\lambda = \frac{h_c}{W_t}$

d. If $I_{yc} / I_y > 0.23$

i. If $\lambda \le \lambda_{pw}$: $R_{pc} = M_p / M_{yc}$

ii. If $\lambda > \lambda_{pw}$: $\lambda_{rw} = 5.7\sqrt{\frac{E}{F_y}}$, $R_{pc} = \left[\frac{M_p}{M_{yc}} - \left(\frac{M_p}{M_{yc}} - 1\right)\left(\frac{\lambda - \lambda_{pw}}{\lambda_{rw} - \lambda_{pw}}\right)\right] \le \frac{M_p}{M_{yc}}$

e. If $I_{yc} / I_y \le 0.23$: $R_{pc} = 1$, $J = 0$

f. Compression flange yielding: $M_{n1} = R_{pc} M_{yc}$

g. L-T buckling: $L_b = L$, $a_w = \frac{h_c W_t}{f_w f_t}$, $h_0 = W_h + f_t$, $r_t = \frac{f_w}{\sqrt{12\left(\frac{h_0}{d} + \frac{a_w W_h^{\,2}}{6 h_0 d}\right)}}$,

$$L_p = 1.1 r_t \sqrt{\frac{E}{F_y}},\ L_r = 1.95 r_t \frac{E}{0.7F_y}\sqrt{\frac{J}{S_{xc}h_0} + \sqrt{\left(\frac{J}{S_{xc}h_0}\right)^2 + 6.76\left(\frac{0.7F_y}{E}\right)^2}}$$

i. If $L_b \le L_p$: $M_{n2} = M_{n1}$

ii. If $L_p < L_b \le L_r$:

$$M_{n2} = C_b\left[R_{pc}M_{yc} - \left(R_{pc}M_{yc} - 0.7F_y S_{xc}\right)\left(\frac{L_b - L_p}{L_r - L_p}\right)\right] \le R_{pc}M_{yc}$$

iii. If $L_b > L_r$: $F_{cr} = \frac{C_b \pi^2 E}{\left(\frac{L_b}{r_t}\right)^2}\sqrt{1 + 0.078\frac{J}{S_{xc}h_0}\left(\frac{L_b}{r_t}\right)^2}$, $M_{n2} = F_{cr} S_{xc} \le R_{pc} M_{yc}$

h. Compression flange local buckling

i. If fl = C: $M_{n3} = M_{n2}$

ii. If fl = NC: $M_{n3} = R_{pc}M_{yc} - \left(R_{pc}M_{yc} - 0.7F_yS_{xc}\right)\left(\frac{\lambda - \lambda_{pf}}{\lambda_{rf} - \lambda_{pf}}\right)$

iii. If fl = S: $k_c = \frac{4}{\sqrt{W_h / W_t}}$, $\lambda = \frac{f_w}{2f_t}$, $M_{n3} = \frac{0.9Ek_cS_{xc}}{\lambda^2}$

i. M_n = minimum of M_{n1}, M_{n2} and M_{n3}

7. If web = S

a. $h_c = W_h$, $S_{xc} = S_{xt} = I_x / (W_h/2 + f_t)$

b. $a_w = \frac{h_cW_t}{f_wf_t} \le 10$, $R_{pg} = 1 - \frac{a_w}{1200 + 300a_w}\left(\frac{h_c}{W_t} - 5.7\sqrt{\frac{E}{F_y}}\right) \le 1.0$

c. Compression flange yielding: $M_{n1} = R_{pg}F_yS_{xc}$

d. L-T buckling: $L_b = L$, $r_t = \frac{f_w}{\sqrt{12\left(\frac{h_0}{d} + \frac{a_wW_h^2}{6h_0d}\right)}}$

$L_p = 1.1r_t\sqrt{\frac{E}{F_y}}$, $L_r = \pi r_t\sqrt{\frac{E}{0.7F_y}}$

i. If $L_b \le L_p$: $M_{n2} = M_{n1}$

ii. If $L_p < L_b \le L_r$: $F_{cr} = C_b\left(F_y - (0.3F_y)\left(\frac{L_b - L_p}{L_r - L_p}\right)\right) \le F_y$

iii. If $L_b > L_r$: $F_{cr} = \frac{C_b\pi^2E}{\left(\frac{L_b}{r_t}\right)^2} \le F_y$

iv. $M_{n2} = R_{pg}F_{cr}S_{xc}$

e. Compression flange local buckling

i. If fl = C: $M_{n3} = M_{n2}$

ii. If fl = NC: $\lambda = f_w / 2f_t$, $\lambda_{pf} = 0.38\sqrt{\frac{E}{F_y}}$, $\lambda_{rf} = \sqrt{\frac{E}{F_y}}$

$$F_{cr} = F_y - (0.3F_y)\left(\frac{\lambda - \lambda_{pf}}{\lambda_{rf} - \lambda_{pf}}\right)$$

iii. If fl = S: $0.35 \le K_c = \frac{4}{\sqrt{h / w_t}} \le 0.76$, $\lambda = \frac{f_w}{2 f_t}$, $F_{cr} = \frac{0.9Ek_c}{\lambda^2}$

iv. If fl = NC or S: $M_{n3} = R_{pg} F_{cr} S_{xc}$

f. M_n = minimum of M_{n1}, M_{n2} and M_{n3}

8. $M_n = M_n / 1.67$

9. Return M_a / M_n

3.2.3b Design checks for flexure (minor axis)

1. Classify the flange

   a. If $\frac{f_w}{2f_t} < 0.38\sqrt{\frac{E}{F_y}}$: section has compact flanges (fl = C)

   b. If $0.38\sqrt{\frac{E}{F_y}} < \frac{f_w}{2f_t} < \sqrt{\frac{E}{F_y}}$: section has non-compact flanges (fl = NC)

   c. If $\frac{f_w}{2f_t} > \sqrt{\frac{E}{F_y}}$: section has slender flanges (fl = S)

2. S_y = elastic section modulus @y-axis

3. Yielding: $M_{n1} = M_p = F_y Z_y \le 1.6\, F_y S_y$

4. Flange local buckling: $\lambda = f_w / 2f_t$

   a. If fl = C: $M_{n2} = M_{n1}$

   b. If fl = NC: $\lambda_{pf} = 0.38\sqrt{\frac{E}{F_y}}$, $\lambda_{rf} = \sqrt{\frac{E}{F_y}}$

   $$M_{n2} = M_p - (M_p - 0.7F_y S_y)\left(\frac{\lambda - \lambda_{pf}}{\lambda_{rf} - \lambda_{pf}}\right)$$

   c. If fl = S: $F_{cr} = \frac{0.69E}{\lambda^2}$, $M_{n2} = F_{cr} S_y$

5. M_n = minimum of M_{n1} and M_{n2}

6. $M_n = M_n / 1.67$

7. Return Ma / Mn

3.2.4 Design Checks for Combined Effect of Axial Force and Bending Moment

1. P_r = axial force acting on the element.
2. M_{rx} = bending moment acting about x-axis.
3. M_{ry} = bending moment acting about y-axis.
4. Depending on the nature of P_r, implement algorithm 4.3.1 to get the axial strength capacity P_c
5. Implement algorithm 4.3.3a to get moment capacity of the beam about x-axis, M_{nx} $M_{cx} = M_{nx}$
6. Implement algorithm 4.3.3b to get moment capacity of the beam about y-axis, M_{ny} $M_{cy} = M_{ny}$
7. If $\frac{P_r}{P_c} \geq 0.2$:

   Return $\frac{P_r}{P_c} + \frac{8}{9}\left(\frac{M_{rx}}{M_{cx}} + \frac{M_{ry}}{M_{cy}}\right)$

8. If $\frac{P_r}{P_c} < 0.2$:

   Return $\frac{P_r}{2P_c} + \frac{M_{rx}}{M_{cx}} + \frac{M_{ry}}{M_{cy}}$

4 DESIGN OPTIMIZATION PROBLEM FORMULATION

4.1 Objective Function, Design Variables and Constraints in general

In general, design optimization problems posed in mathematical programming format are usually of the following form. [6]

Find $\mathbf{x} \in R^n$

To minimize $f(\mathbf{x})$

Subject to $g_i(\mathbf{x}) \le 0 \qquad i = 1, 2, \ldots l \qquad (4.1.1)$

$h_j(\mathbf{x}) = 0 \qquad j = 1, 2, \ldots m \qquad (4.1.2)$

$x_k^L \le x_k \le x_k^U \qquad k = 1, 2, \ldots n \qquad (4.1.3)$

In the above equations, $\mathbf{x}$ represents the vector of design variables. The notation $\mathbf{x} \in R^n$ indicates that the design variables are real-valued and that there are *n* variables, $x_1, x_2, \ldots x_n$. The function $f(\mathbf{x})$ is the objective function and is either directly or indirectly the function of *n* design variables.

Performance requirements, manufacturing requirements, and/or permissible range of values for certain design variables can be specified through constraints. The constraints $g_i(\mathbf{x})$ are inequality constraints and $h_j(\mathbf{x})$ are equality constraints. Constraints described in equation 4.1.3 are typical lower-upper bound constraints, usually referred to as bound constraints. A problem posed in the above form is called as *constrained minimization problem*.

4.2 Types of design variables

The types of design variables being used are *discrete design variables*, *continuous design variables* and *Boolean variables*.

Discrete design variables (DDV) are the type of variables that are available in 'discrete' or predefined sets of values. For example, standard hot-rolled steel sections defined in AISC 2010 manual, certain allowable locations of nodes in a structure, available types of material for a construction project.

Continuous design variables (CDV) vary continuously over the predefined range. Dimensions of a plate girder or a concrete beam, location of nodes in a structure are a few examples of CDV's.

Boolean variables (BV) also known as *zero-one* design variables. These variables can either have a value 0 or 1. These variables are implemented generally to specify the presence (value of 1) or absence (value of 0) of an element in a structure.

Types of constraints

There are two types of constraints, namely, equality and inequality constraints.

Equality constraints are used to define relationships between two or more design variables using the 'equality' operator. For example, we can define the symmetry requirements of a structure by enforcing constraint(s) for node locations.

Inequality constraints are used to express relationship between two or more design variables using either a 'greater than', 'less than', 'greater than or equal to' or 'less than or equal to' operators. For example, we can implement the requirements of stresses in elements to be less than or equal to a certain value, limit maximum deflections of node(s), so on and so forth.

In general, structural engineering problems have a single objective function. Either minimize the weight or volume of the structure, cost of the project, or minimize the deflection.

Using the different types of variables, constraint functions and objective functions, it is possible to pose various types of mathematical programming problems. Most engineering problems that require constraints be satisfied are defined as *Nonlinear Programming (NLP) problem.* Usually, the vector $\mathbf{x}$ is defined with multiple aforementioned types of design variables.

The objective is to find a set of values for vector $\mathbf{x}$ such that the objective function has, generally , the lowest possible value without violating the constraints.

4.3 Regression Analysis

The variables in a design optimization problem are the element sizing variables and topological variables. If only sizing optimization is considered in a particular case, then the topology is presumed to be fixed. Element sizing variables vary the cross-sectional properties of structural elements. They can be continuous, or discrete. In practical structural design, steel structures use standard AISC sections which are discrete variables or built–up sections which are continuous variables.

Structural design optimization using discrete design variables is found to be time expensive. This is essentially due to the discontinuities among the various properties of element cross-sections. Even well-established methods which work with DDVs like Genetic algorithm (GA) and Differential evolution (DE) take a lot of time to arrive at a well performing design. Whereas, Method of Feasible Direction (MFD) algorithm performs much faster as compared to GA or DE. To quantify this, GA or DE takes ~20

minutes to optimize a 10 storied planar frame and MFD does the same job within a minute. The only issue with MFD is that it cannot work with DDV type of variables.

Hence, to be able to use MFD for optimization purposes, we define 'user-defined general cross sections' with all parameters necessary for the design process as a function of c/s area.

In AISC design checks, I_{zz} values are of most importance since most of the limit states are a function of I_{zz}. All available 273 cross-sections in AISC database were examined for relationships between the cross sectional area and various parameters, most importantly I_{zz}. It was found that there were sections with lower I_{zz} values for a given area. 84 out of 273 such sections were not selected to establish the relationships. Following graphs illustrate the I_{zz} distribution throughout the selected database and the curve fitting through these values.

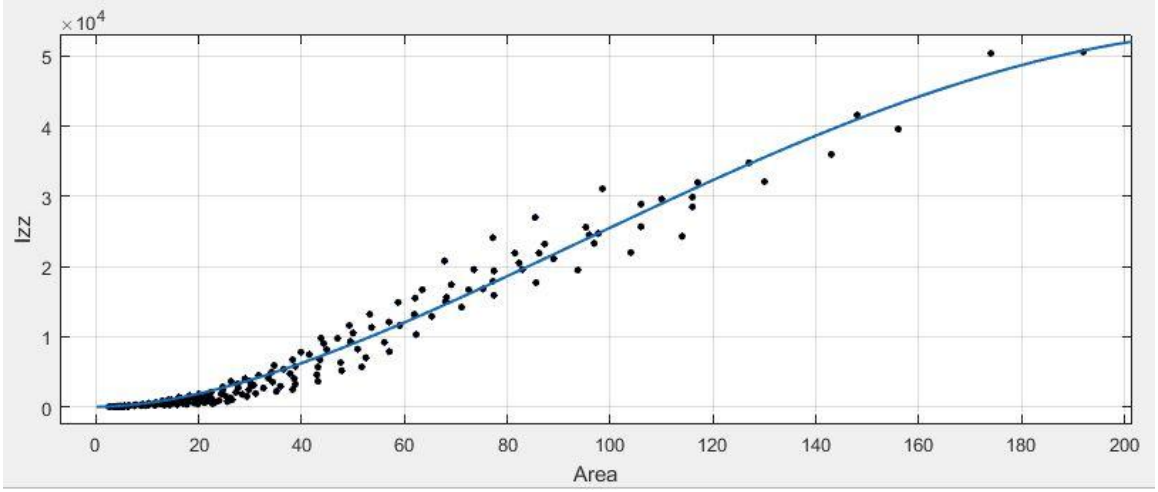

Figure 4.1 Regression analysis : Area vs I_{zz}

The relationships and R^2 values obtained from this exercise for various parameters required for the design process are as follows.

Parameter	Function	R^2
I_{zz}	$14.01A^{2.07} - 7.361A^{2.179}$	0.972
S_{zz}	$4.576A^{1.216}$	0.9827
I_{yy}	$1.261A^{1.492}$	0.9422
S_{yy}	$0.4183A^{1.287}$	0.9675
J	$0.0002963A^{2.757}$	0.9959
SF_{zz}	$0.1942A - 0.001206$	0.9833
SF_{yy}	$0.3767A - 0.1297$	0.9789
TF	$0.009332A^{1.887}$	0.9958

Table 4.1 C/S properties as a function of Area

After arriving at an optimal design, the area of a general section design variable can be used to select appropriate AISC cross sections for all the elements such that the area of the AISC section is larger than the user defined section.

4.4 Optimization Solution Techniques

When there are multiple types of variables present in the design optimization problem, the problem is solved in stages. First, the problem is treated as a sizing optimal design problem. Only sizing parameters are treated as the design variables. Of course, in doing this, it is required to assume certain values for the shaping and topology variables. These assumed values need to be the designers call, and are usually based on experience.

Once we arrive at the optimal design based on sizing variables, the problem is treated as a combined sizing and shape optimal design problem. Meaning, the shape parameters are added to the design vector. The upper and lower bounds of shape optimal design variables are adjusted so that, more or less, these values lie in the center of the bounds. Now, as number of design variables increase, it is necessary to increase the population size. We start with the solution from feasible-optimal size design and arrive at feasible-optimal size and shape design.

Similarly, and finally, we treat the design problem as a combined sizing, shape and topology design optimization problem. Again, we start with the sizing and shape design parameters obtained in previous step. The bounds of design variables are readjusted so as their values lie in the center. On arriving at an optimal design from this procedure, the values of variables are rechecked to see if bound confinement is in effect. Meaning, if the values are close to lower or upper bounds. If so, the bounds are adjusted again, and the problem is rerun. In Frame3D, for a design to be feasible, all the constraint values evaluated, need to be less than or equal to zero.

4.5 Design optimization problem formulation - MWD

The objective function in all the cases is to minimize the weight of the structure. This type of a problem is referred to as *Minimum Weight Design problem.* All the structures are being designed with two different types of constraints, strength based constraints and AISC 2010 constraints.

MWD problem with strength based constraints

Find $\mathbf{x} \in \{\mathbf{x}_{cdv}, \mathbf{x}_{ddv}\}$

To minimize $W(\mathbf{x}) = \sum_{i=1}^{n} A_i L_i \gamma_i$

Subject to

$$\sigma_{\max,i}^{t,c} \le \sigma_a^{t,c} \qquad i = 1, 2, \ldots l \qquad (4.3.1)$$

$$\tau_{\max,i} \le \tau_a \qquad i = 1, 2, \ldots l \qquad (4.3.2)$$

$$(D_i)_{\max}^{T} \le D_a \qquad i = 1, 2, \ldots m \qquad (4.3.3)$$

$$\frac{D_j - D_{j-1}}{h_j} \le (D_{ij})_a \qquad j = 1, 2, \ldots m \qquad (4.3.4)$$

$$\lambda^B \ge \lambda_a^B \qquad (4.3.5)$$

$$\mathbf{x}_{(ddv)\mathbf{k}}^{\mathbf{L}} \le \mathbf{x}_{(ddv)\mathbf{k}} \le \mathbf{x}_{(ddv)\mathbf{k}}^{\mathbf{U}} \qquad k = 1, 2, \ldots n \qquad (4.3.6)$$

$$\mathbf{x}_{(cdv)\mathbf{k}}^{\mathbf{L}} \le \mathbf{x}_{(cdv)\mathbf{k}} \le \mathbf{x}_{(cdv)\mathbf{k}}^{\mathbf{U}} \qquad k = 1, 2, \ldots n \qquad (4.3.7)$$

where W is the total weight of structure, γ_i is the weight density of material, L_i is the length and A_i is the cross-sectional area of member i. Equations (4.3.1) and (4.3.2) are used to impose stress constraints where $\sigma_{\max,i}^{t}$, $\sigma_{\max,i}^{c}$, $\tau_{\max,i}$ are the maximum tensile, compressive and shear stress, and the subscript a denotes the allowable value.

Equation (4.3.3) defines the constraints imposed on the maximum lateral drift $(D_i)^T_{\max}$ in longitudinal and transverse directions of the building. Equation (4.3.4) defines the inter-story drift constraints for the structure where D_j and D_{j-1} are the drifts of j^{th} and $(j-1)^{th}$ story respectively and h_j is the height of j^{th} story. Buckling constraints are imposed via Equation (4.3.5) in the form of overall buckling of the structure where λ^B is the lowest Eigenvalue from the buckling Eigenvalue problem and λ_a^B is the allowable value. Eqn. (4.3.6) is used to denote discrete design variables (selected from a predetermined table of cross-sectional shapes) and Equation (4.3.7) is used to denote continuous design variables as explained earlier.

Stress Constraints

Strength based design requirements are imposed where the requirement is that the allowable strength of each structural component equals or exceeds the required strength. As per AISC Specification (2005), the allowable tensile/compressive stress for gross steel cross section is $0.6 f_y$ and the allowable shear stress for gross steel cross section is $0.4 f_y$ where f_y is the yield strength of the steel material. In the finite element analysis, the magnitude of the maximum beam element stresses is computed conservatively as follows (x-y-z denote the longitudinal axis and the two transverse directions, respectively) at the two ends and at the quarter-points of each beam finite element.

Normal stress

$$\sigma^t_{\max} = \max\left(\frac{N_x}{A} + \frac{|M_y|}{S_y} + \frac{|M_z|}{S_z}, 0\right) \tag{15}$$

$$\sigma_{\max}^{c} = \min\left(\frac{N_x}{A} - \frac{|M_y|}{S_y} - \frac{|M_z|}{S_z}, 0 \right) \tag{16}$$

Shear stress

$$\tau^y = \frac{|V_y| Q_y}{I_y t_y} \qquad \tau^z = \frac{|V_z| Q_z}{I_z t_y} \qquad \tau^T = \frac{|T_x|}{T_J} \tag{17}$$

$$\tau_{\max} = \max\left\{ \tau^y + \tau^T, \tau^z + \tau^T \right\} \tag{18}$$

where $\left\{ A, S_y, S_z, Q_y, Q_z, t_y, t_z, I_y, I_z, T_J \right\}$ are the cross-sectional properties and dimensions, i.e. area, section moduli, first moments of the area, widths resisting shear, moments of inertia and torsional constant, respectively, $\left\{ N_x, V_y, V_z \right\}$ are the normal and shear forces in the element's local x, y, z directions, and $\left\{ T_x, M_y, M_z \right\}$ are the torsional and bending moments in the element's local x, y, z directions.

Displacement Constraints

Two types of displacement constraints are imposed – Equations (4.3.3) and (4.3.4). First, the displacements in the two transverse directions are limited to 1/600 to 1/400 of the total building height [ASCE, 1998]. Second, the inter-story drift is another serviceability criterion for design requirements is taken to be less than 1/500 of the story height [Ng and Lam, 2005].

Buckling Constraints

In addition of the strength requirements imposed via stress constraints, in performance based designs, structural instability must be prevented. Buckling behavior of the structure is determined by solving the Eigenvalue problem described in section 2.2,

where λ^B is the lowest buckling load factor that needs to be greater than 1 to prevent buckling under the action of the applied loads, i.e. for all load cases.

MWD problem with AISC 2010 constraints

Find $\mathbf{x} \in \{\mathbf{x}_{cdv}, \mathbf{x}_{ddv}\}$

To minimize $W(\mathbf{x}) = \sum_{i=1}^{n} A_i L_i \gamma_i$

Subject to $AISC_i^j \le 0$ $i = 1, 2, \ldots l, j = 1, 2, \ldots 8$ (4.3.8)

$(D_i)_{\max}^T \le D_a$ $i = 1, 2, \ldots m$ (4.3.9)

$\frac{D_j - D_{j-1}}{h_j} \le (D_{ij})_a$ $j = 1, 2, \ldots m$ (4.3.10)

$\lambda^B \ge \lambda_a^B$ (4.3.11)

$\mathbf{x}_{(ddv)\mathbf{k}}^{\mathbf{L}} \le \mathbf{x}_{(ddv)\mathbf{k}} \le \mathbf{x}_{(ddv)\mathbf{k}}^{\mathbf{U}}$ $k = 1, 2, \ldots n$ (4.3.12)

$\mathbf{x}_{(cdv)\mathbf{k}}^{\mathbf{L}} \le \mathbf{x}_{(cdv)\mathbf{k}} \le \mathbf{x}_{(cdv)\mathbf{k}}^{\mathbf{U}}$ $k = 1, 2, \ldots n$ (4.3.13)

Equation (4.3.8) defines the AISC 2010 constraints described in Chapter 3. By implementing this constraint, every element in the finite element model undergoes 8 design checks. The limiting value of every design check is calculated as a function of the section properties, length, and forces and moments acting on the element. All other constraints are imposed as defined previously.

5 VALIDATION OF FEA (with ABAQUS)

Before we proceed to case studies for studying the techniques discussed earlier in this dissertation, it is necessary to validate Frame3D results. For this purpose, results from Frame3D of a few models are compared with those from Abaqus. Types of analyses being verified include stress (static) analysis and modal (frequency) analysis. Responses from the following planar and 3D models are compared using Frame3D (V 2.83) and Abaqus (6.11-1).

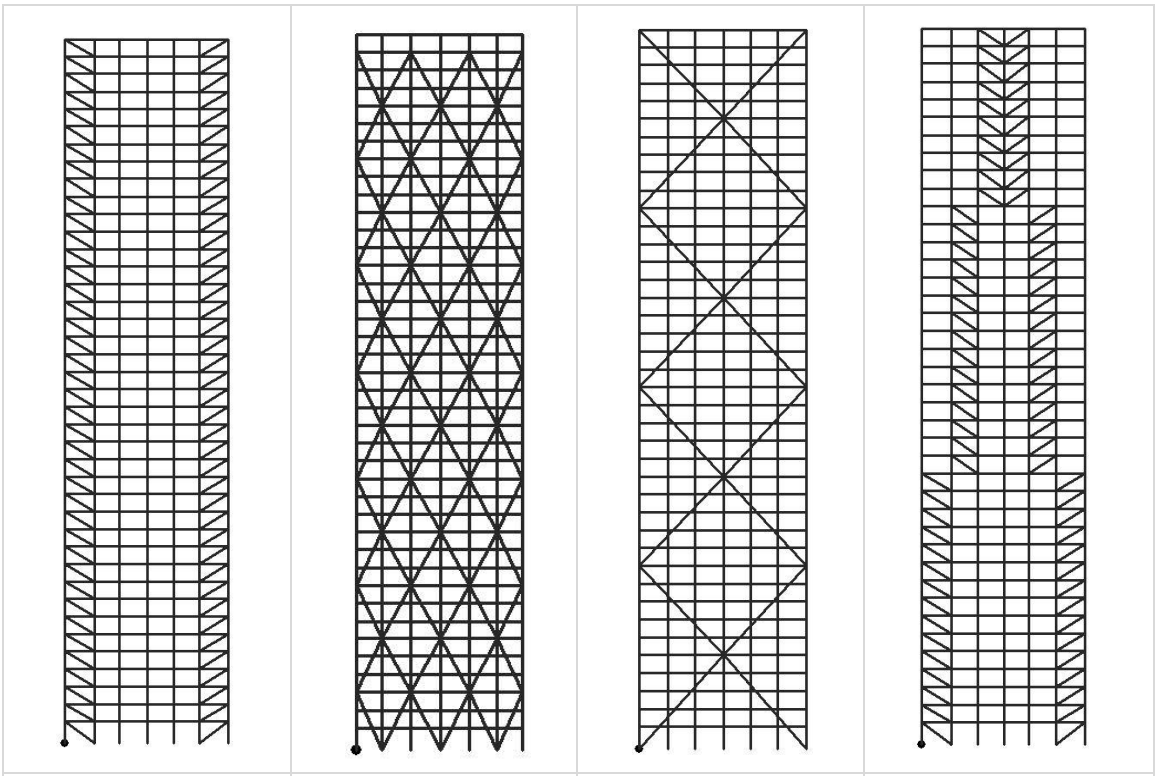

40S-PL_Bay1	40S-PL_DG	40S-PL_FT	40S-PL_Pyramid

Figure 5.1 Models for validation of Frame3D

5.1 Static Analysis

Since it is not feasible to include results for all nodes and elements from all the models, results in the form of highest values of nodal displacements (which occur at the topmost point in a structure), nodal reactions at two nodes, and randomly selected elements for beam element forces & moments are being observed. Results from load cases (i) dead load + live load (LC1) and (ii) dead, live + 0.6 wind loads (LC4) are being compared. Following tables illustrate the observations.

Displacement comparison - Load case 1 - Dead load + Live load							
Model Name	Node	Abaqus			Frame3D		
		X-Disp	Z-Disp	Y-Rot	X-Disp	Z-Disp	Y-Rot
		in	*in*	*rad*	*in*	*in*	*rad*
40S-PL-DV+CV-D+L+W_AISC_Bay1	41-7	-7.96E-02	-3.35	-2.21E-03	-7.96E-02	-3.35	-2.20E-03
	41-1	7.96E-02	-3.35	2.21E-03	7.96E-02	-3.35	2.20E-03
40S-PL-DV+CV-D+L+W_AISC_DG	41-7	1.99E-02	-3.10	1.72E-03	1.99E-02	-3.10	1.72E-03
	41-1	-1.93E-02	-3.10	-1.72E-03	-1.93E-02	-3.10	-1.72E-03
40S-PL-DV+CV-D+L+W_AISC_FT	41-7	2.23E-02	-3.21	3.74E-03	-2.23E-02	-3.21	-3.73E-03
	41-1	-2.23E-02	-3.21	-3.74E-03	2.23E-02	-3.21	3.73E-03
40S-PL-DV+CV-D+L+W_AISC_Pyr	41-7	3.76E-02	-3.15	8.26E-04	-3.76E-02	-3.15	-8.26E-04
	41-1	-3.75E-02	-3.15	-8.26E-04	3.76E-02	-3.15	8.26E-04

Table 5.1 Nodal displacements – LC1

Displacement comparison - Load case 2 - Dead load + 0.6 wind load							
Model Name	Node	Abaqus			Frame3D		
		X-Disp	Z-Disp	Y-Rot	X-Disp	Z-Disp	Y-Rot
		in	*in*	*rad*	*in*	*in*	*rad*
40S-PL-DV+CV-D+L+W_AISC_Bay1	41-7	1.02E+01	-2.33	1.65E-04	1.01E+01	-2.33	1.65E-04
	41-1	1.02E+01	-1.30	2.48E-03	1.02E+01	-1.30	2.48E-03
40S-PL-DV+CV-D+L+W_AISC_DG	41-7	4.10E+00	-2.08	-3.53E-04	4.10E+00	-2.08	-3.50E-04
	41-1	4.12E+00	-1.29	1.43E-03	4.12E+00	-1.29	1.43E-03
40S-PL-DV+CV-D+L+W_AISC_FT	41-7	4.69E+00	-1.29	2.99E-03	4.69E+00	-1.29	2.98E-03
	41-1	4.67E+00	-2.23	-1.33E-03	4.67E+00	-2.23	-1.33E-03
40S-PL-DV+CV-D+L+W_AISC_Pyr	41-7	8.39E+00	-2.18	2.62E-04	8.38E+00	-2.18	2.62E-04
	41-1	8.43E+00	-1.24	1.13E-03	8.42E+00	-1.24	1.13E-03

Table 5.2 Nodal displacements – LC4

Reaction comparison - Load case 1 - Dead load + live load							
Model Name	Node	Abaqus			Frame3D		
		X-Force	Z-Force	Y-Mom	X-Force	Z-Force	Y-Mom
		lb	*lb*	*lb-in*	*lb*	*lb*	*lb-in*
40S-PL-AISC_Bay1	1	9.09E+03	1.89E+06	7.48E+05	9.10E+03	1.89E+06	7.50E+05
	2	-1.58E+04	2.25E+06	2.03E+05	-1.58E+04	2.25E+06	2.03E+05
40S-PL-AISC_DG	1	1.52E+03	1.84E+06	1.28E+06	1.53E+03	1.84E+06	1.28E+06
	2	4.11E+04	2.40E+06	9.29E+05	4.11E+04	2.40E+06	9.32E+05
40S-PL-AISC_FT	1	1.88E+05	2.10E+06	2.03E+05	1.88E+05	2.10E+06	9.18E+04
	2	-3.51E+02	2.19E+06	1.29E+04	-3.49E+02	2.19E+06	1.31E+04
40S-PL-AISC_Pyr	1	2.08E+04	1.83E+06	2.20E+06	2.08E+04	1.83E+06	2.20E+06
	2	-4.80E+04	2.25E+06	3.53E+05	-4.80E+04	2.25E+06	3.53E+05

Table 5.3 Nodal reactions – LC1

Reaction comparison - Load case 4 - Dead load + 0.6 wind load							
Model Name	Node	Abaqus			Frame3D		
		X-Force	Z-Force	Y-Mom	X-Force	Z-Force	Y-Mom
		lb	*lb*	*lb-in*	*lb*	*lb*	*lb-in*
40S-PL-AISC_Bay1	1	-2.49E+04	4.22E+05	-4.30E+06	-2.49E+04	4.22E+05	-4.31E+06
	2	-5.73E+04	1.32E+06	-5.05E+06	-5.73E+04	1.32E+06	-5.06E+06
40S-PL-AISC_DG	1	-1.07E+04	5.75E+05	-2.66E+06	-1.08E+04	5.75E+05	-2.66E+06
	2	-5.26E+04	1.07E+06	-2.87E+06	-5.26E+04	1.07E+06	-2.88E+06
40S-PL-AISC_FT	1	-5.58E+03	6.31E+05	-2.05E+06	-5.42E+03	6.31E+05	-2.06E+06
	2	-1.00E+04	1.06E+06	-2.02E+06	-1.00E+04	1.06E+06	-2.02E+06
40S-PL-AISC_Pyr	1	-6.86E+02	2.68E+05	-2.11E+06	-6.74E+02	2.69E+05	-2.11E+06
	2	-8.27E+04	1.43E+06	-4.69E+06	-8.27E+04	1.43E+06	-4.70E+06

Table 5.4 Nodal reactions – LC4

Axial force and moment - Load case 1 - Dead load + live load						
Model Name	Element	Node	Abaqus		Frame3D	
			Axial	Z-Moment	Axial	Z-Moment
			lb	*lb-in*	*lb*	*lb-in*
40S-PL_AISC_Bay1	1C-1	7	-1.89E+06	7.48E+05	1.89E+06	7.50E+05
		84	-1.89E+06	-9.97E+05	-1.89E+06	9.97E+05
	1C-7	1	-1.89E+06	-7.48E+05	1.89E+06	-7.50E+05
		78	-1.89E+06	9.97E+05	-1.89E+06	-9.97E+05
40S-PL_AISC_DG	1C-1	7	-1.84E+06	1.28E+06	1.84E+06	1.28E+06
		84	-1.84E+06	9.92E+05	-1.84E+06	-9.92E+05
	1C-7	1	-1.84E+06	-1.28E+06	1.84E+06	-1.28E+06
		78	-1.84E+06	-9.91E+05	-1.84E+06	9.92E+05
40S-PL_AISC_FT	1C-1	7	-1.89E+06	5.41E+05	1.89E+06	5.42E+05
		84	-1.89E+06	-8.16E+05	-1.89E+06	8.16E+05
	1C-7	1	-1.89E+06	-5.41E+05	1.89E+06	-5.42E+05
		78	-1.89E+06	8.16E+05	-1.89E+06	-8.16E+05
40S-PL_AISC_Pyramid	1C-1	7	-1.83E+06	-2.20E+06	1.83E+06	2.20E+06
		84	-1.82E+06	1.79E+06	-1.82E+06	1.80E+06
	1C-7	1	-1.83E+06	2.20E+06	1.83E+06	-2.20E+06
		78	-1.82E+06	-1.79E+06	-1.82E+06	-1.80E+06

Table 5.5 Beam forces and moments – LC1

Axial force and moment - Load case 2 - Dead load + 0.6 wind load						
Model Name	Element	Node	Abaqus		Frame3D	
			Axial	Z-Moment	Axial	Z-Moment
			lb	*lb-in*	*lb*	*lb-in*
40S-PL_AISC_Bay1	1C-1	7	-4.22E+05	4.24E+06	4.22E+05	-4.31E+06
		84	-4.16E+05	-1.67E+05	-4.16E+05	-1.00E+05
	1C-7	1	-1.67E+06	5.04E+06	1.67E+06	-5.11E+06
		78	-1.67E+06	-1.24E+06	-1.67E+06	-1.17E+06
40S-PL_AISC_DG	1C-1	7	-5.75E+05	2.60E+06	5.75E+05	-2.66E+06
		84	-5.69E+05	9.01E+05	-5.69E+05	9.64E+05
	1C-7	1	-1.46E+06	3.98E+06	1.46E+06	-4.05E+06
		78	-1.46E+06	2.03E+06	-1.46E+06	2.09E+06
40S-PL_AISC_FT	1C-1	7	-6.28E+05	1.55E+06	6.27E+05	-1.62E+06
		84	-6.22E+05	8.74E+05	-6.22E+05	9.38E+05
	1C-7	1	-1.48E+06	2.12E+06	1.48E+06	-2.19E+06
		78	-1.48E+06	1.06E+04	-1.48E+06	7.38E+04
40S-PL_AISC_Pyramid	1C-1	7	-2.68E+05	2.05E+06	2.69E+05	-2.11E+06
		84	-2.62E+05	2.29E+06	-2.63E+05	2.35E+06
	1C-7	1	-1.75E+06	4.45E+06	1.75E+06	-4.52E+06
		78	-1.75E+06	3.42E+05	-1.75E+06	4.06E+05

Table 5.6 Beam forces and moments – LC4

5.2 Modal Analysis

Following tables illustrate the natural frequency, fundamental periods and modal Eigenvalues of said models.

Model	Abaqus			Frame3D			Total mass	
	Mode 1	Mode 2	Mode 3	Mode 1	Mode 2	Mode 3	Abaqus	Frame3D
	Hz						*lbm*	
(Nodal) Point Masses Using Dead plus Live Loads								
40S-Bay1	0.166	0.504	0.920	0.166	0.505	0.920	38780.5	38780.5
40S-DG	0.262	0.830	1.547	0.262	0.830	1.547	38834.0	38834.0
40S-FT	0.243	0.806	1.390	0.243	0.806	1.390	39094.1	39094.1
40S-Pyramid	0.176	0.552	0.908	0.176	0.552	0.908	38777.4	38777.4

Table 5.7 Lowest frequencies

Model	Abaqus			Frame3D			Total mass	
	Mode 1	Mode 2	Mode 3	Mode 1	Mode 2	Mode 3	Abaqus	Frame3D
	Seconds						*lbm*	
(Nodal) Point Masses Using Dead plus Live Loads								
40S-Bay1	6.028	1.982	1.087	6.025	1.982	1.086	38780.5	38780.5
40S-DG	3.824	1.205	0.646	3.824	1.205	0.646	38834.0	38834.0
40S-FT	4.118	1.240	0.720	4.118	1.240	0.719	39094.1	39094.1
40S-Pyramid	5.681	1.811	1.102	5.679	1.810	1.102	38777.4	38777.4

Table 5.8 Highest fundamental periods

Model	Abaqus			Frame3D		
	Modal Eigenvalues					
	1	2	3	1	2	3
(Nodal) Point Masses Using Dead plus Live Loads						
40S-Bay1	1.086	10.045	33.419	1.087	10.054	33.448
40S-DG	2.700	27.188	94.496	2.700	27.187	94.498
40S-FT	2.328	25.668	76.237	2.328	25.671	76.281
40S-Pyramid	1.223	12.041	32.514	1.224	12.047	32.529

Table 5.9 Modal Eigenvalues

It is observed that all the three types of analyses results are in close agreement with Abaqus results. Highest variation in any type of results is observed to be less than 1%.

5.3 Redundancy of Nonlinear Geometric Analysis

All the models being analyzed and/or designed in this dissertation, with strength based constraints and with AISC 2010 constraints, stresses in all elements are within the elastic limit of the material. Since the inelastic behavior of the material is not being considered it is not required to perform a nonlinear geometric analysis. Moreover, since all the displacements are within the specified limits, this also adds to unnecessity of nonlinear geometry.

6 DESIGN OPTIMIZATION CASE STUDIES

6.1 Finite Element Model

All design models are constructed using a three dimensional, two node beam element formulation with six independent degrees of freedom (three translations and three rotations) at each end node of the element. All beams, columns and bracings are modelled using this type of element. Frame3D uses a 3rd node to define the orientation of the cross section of the said beam element. Following figures show the degrees of freedom in local coordinate system in a typical beam element and usage of a 3rd node to define orientation. All structures are being modelled in US customary units [Units – *lb, lbm, in, psi*].

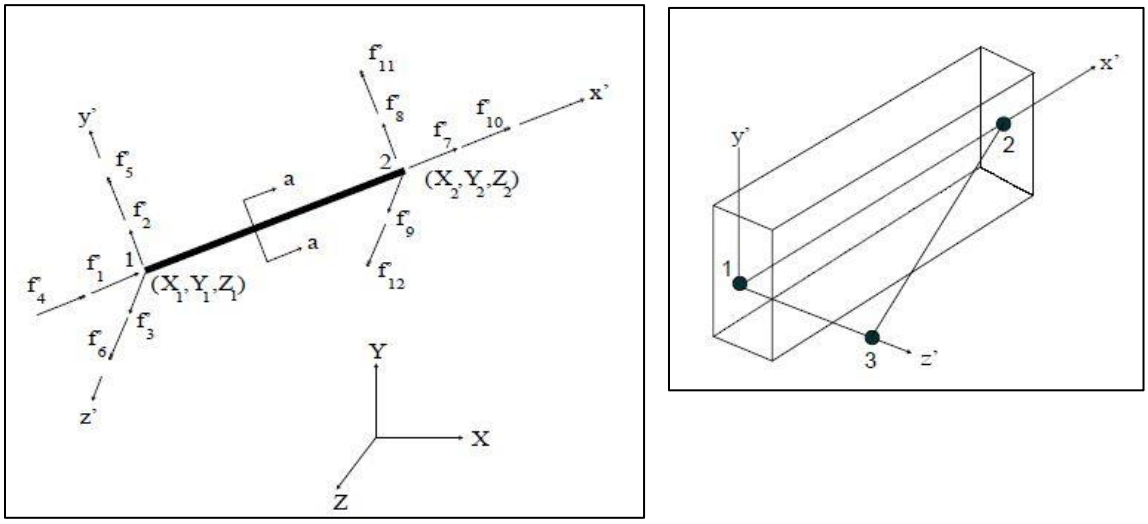

Figure 6.1 Space beam element description and orientation using a 3rd node

Frame3D computer program is employed so as to carry out static analysis, Eigenvalue buckling analysis, modal analysis and optimal design (using stated analyses) of interior and exterior planar frames of a square-in-plan building, utilizing only beam elements. A basic flowchart of the design process implemented in the Frame3D program, is shown below.

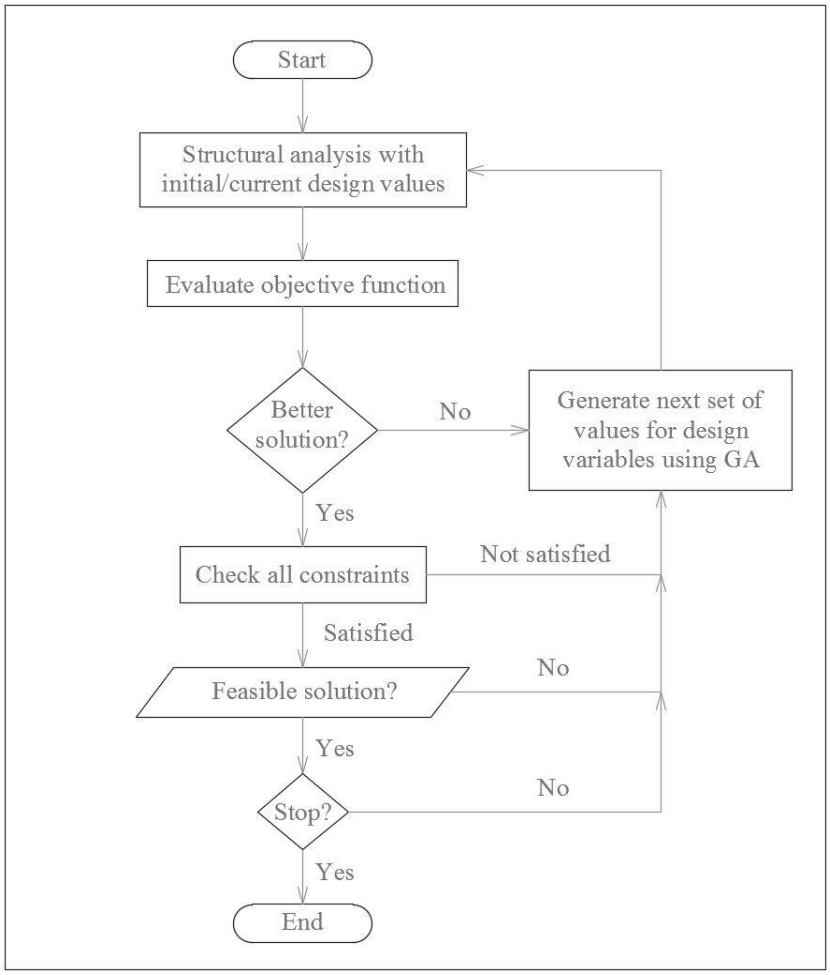

Figure 6.2 Flowchart of the design process

6.1.1 Building Layout

The constructed design methodology is tested for designing 10, 20, 40 and 60 storey buildings. All structurers are modelled as planar frames, with a rectangular floor layout of aspect ratio 1:1. These frames are assumed to be part of a 3D structure with a frame spacing, '*S*' of 20 ft. The height of the first floor containing the lobby is 16 ft. and all other subsequent storeys are 13 ft. tall. The floor system consists of a composite metal deck slab (16 gage, 3" cellular steel deck with 5.5" concrete slab), supported on the steel joists. Base columns are assumed to be fixed in all directions. All models are assumed to be symmetrical along grid 'D' (figure 6.1.1)

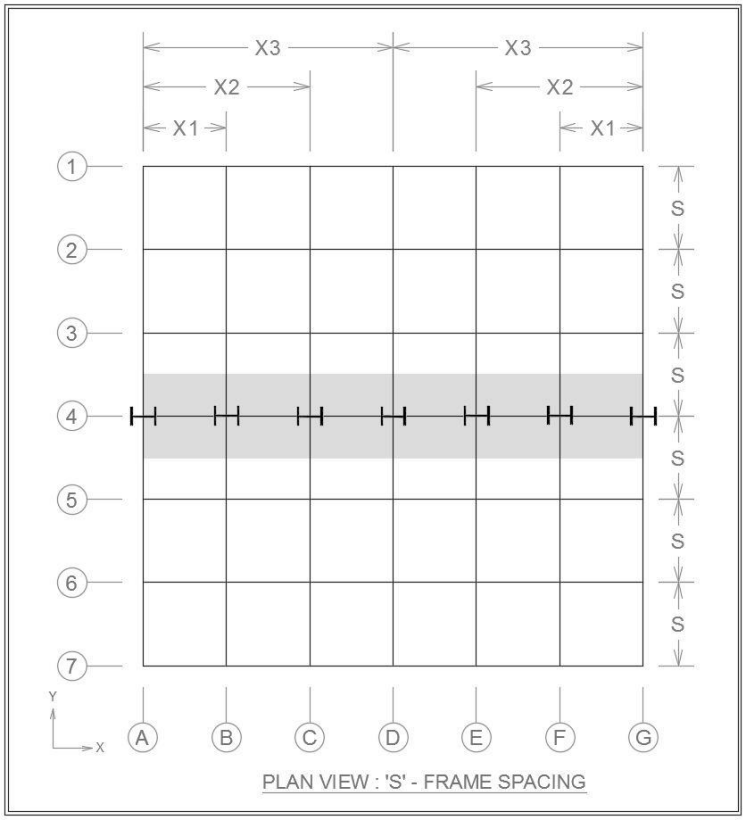

Figure 6.3 Typical building plan

As it was observed in both interior and exterior cases, the extreme end columns were controlling the design and the interior columns were not being utilized fully. To put it in other words, extreme end columns could be designed differently (using a different design variable). But this resulted in increase in the number of design variables and hence increase in the required design duration. Observing that there was already a heavier design available for a lower storey interior column, the exterior columns were modelled same as the interior columns of a group below. Only the columns of bottommost two storeys were typical throughout the floor. This idea is illustrated in figure 6.1.2.

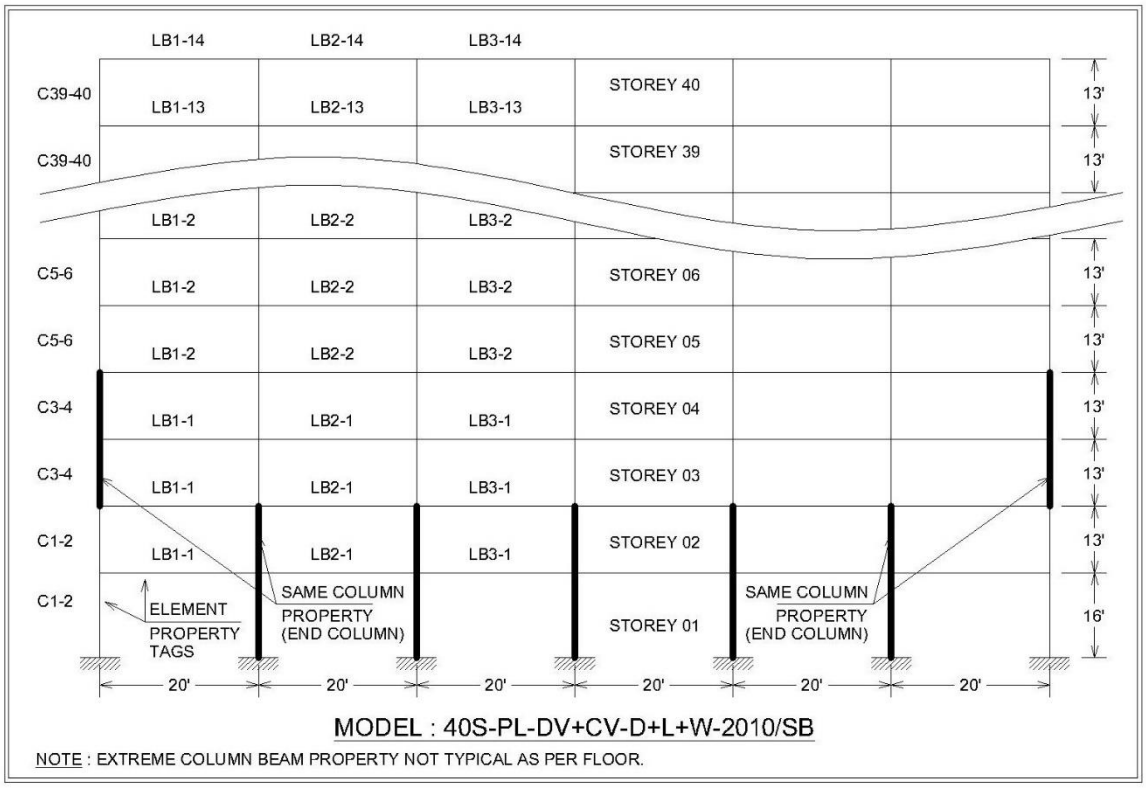

Figure 6.4 Typical elevation of an interior frame

(2010 – AISC constraints, SB – strength based design)

Model	Floors	Beams	Columns	Building Height *(ft)*
10F-Int/Ext-Strength/AISC	10	60	70	133
20F-Int/Ext-Strength/AISC	20	120	140	263
40F-Int/Ext-Strength/AISC	40	240	280	523
60F-Int/Ext-Strength/AISC	60	360	420	783

Table 6.1 General model information

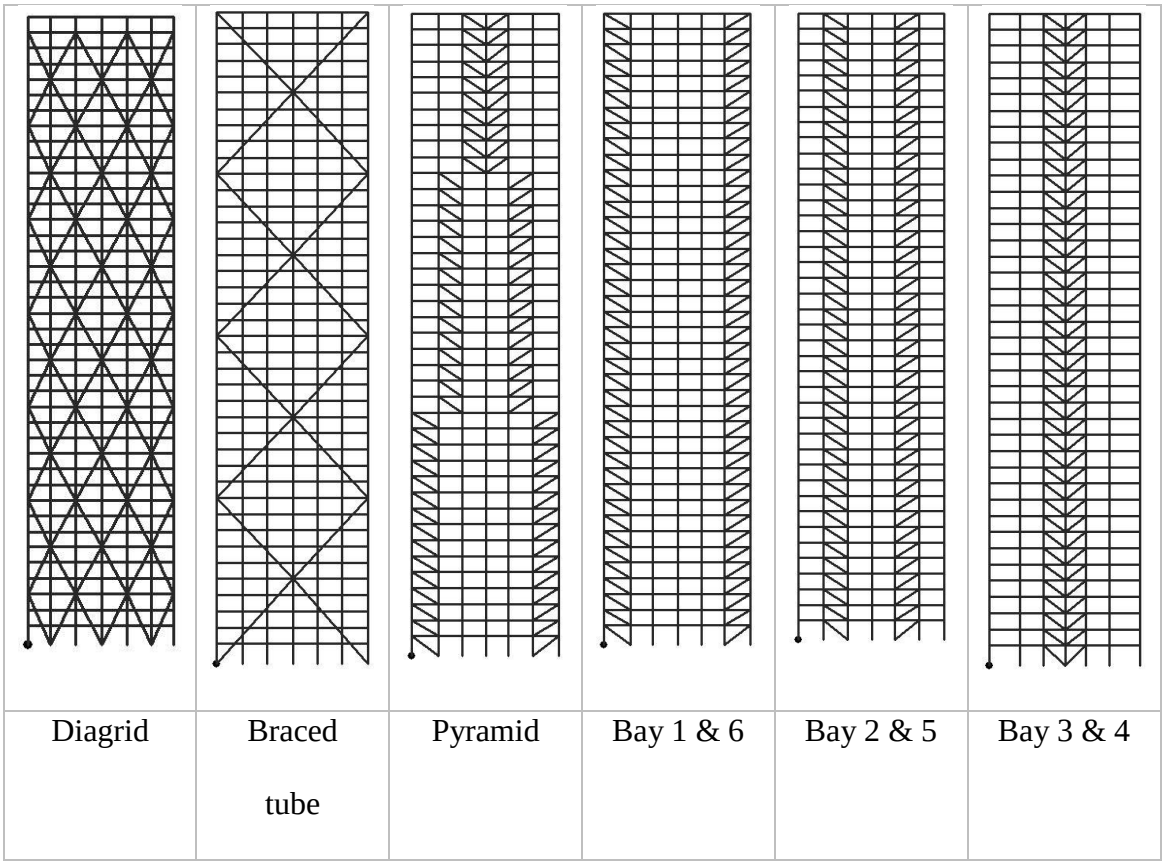

Figure 6.5 Types of bracing systems (typical) for exterior frames

Table 6.1 shows the number of structural members and building height. Figure 6.5 elevations (for 40F) illustrate typically the types of bracing systems under study for all 10, 20, 40 and 60F exterior frames.

6.2 Nomenclature and bracing systems

As mentioned earlier, interior and exterior planar frames of four models are being designed. For every two storeys, there is one column design variable. For example, element property tag for columns of 3rd and 4th storey will be *'c3_4'*. For beam elements, the grouping is done bay-wise. There are 6 symmetrical bays present in all models, this results in 3 bay groups. In the cases of 10F, 20F and 40F models, one variable for one bay and three stories is being defined and that in 60F models, one variable per bay and 4 stories. For example, in a 20F model, there are 5 groups storey-wise and 3 groups bay-wise. *'b2_5'* implies that this variable is defined for second bay, storey-wise 5th group. All these variables are of discrete type.

As seen in figure 6.1.3, there are two shape variables in a model, namely X_1 and X_2. These are continuous design variables, which represent the spans of the bays. X_1 is allowed to vary from 192 to 288 *in* and X_2 from 432 to 528 *in*. Initially, these variables are given a value of 240 and 480 *in*, respectively. As it is a common practice for outermost bays to be wider than the internal bays, a constraint defining this property is also being implemented.

As far as bracing systems for exterior frames are concerned, 6 different types are being studied, namely, Diagrid, Framed Tube, Pyramid type bracing, bay 1 & 6 full, bay 2 & 5 full and bay 3 & 4 all stories braced. Kyoung Sun Moon [10] carried out a study on Diagrids and Framed Tube bracing system. It was observed that optimum angles for structures up to 50 stories for diagrid elements is 63° from horizontal and that for structures higher that 50 stories, was found to be 69°. This was achieved by creating diagrid elements for every 3 stories in the case of 10, 20 and 40 storied models and in the

case of 60 storey, for every 4 stories. It should be noted that since performance of diagrid systems is a function of the angle formed by diagrids, shape optimization was not performed on these systems. They also observed that for framed tube, the optimum angle was 47°. This was achieved by defining the elements for every 5 stories. For pyramid type system, the building was necessarily divided in three parts. The bottom third has bracing elements in the outermost bays, middle third of the height has the bracing elements in intermediate bays and top third in the central two bays. This was done by observing the bending moment throughout the height of the structure.

All beam and column elements are named in a self-explanatory fashion, storey number – beam or column tag – Bay number, e.g. 1-C1, 6-B5 etc. Similarly, the bracing elements are named as, storey number – bracing tag – positive or negative slope – bay number. For example, a bracing element in second bay of fifth storey with a positive slope will have a tag '*5-x1-2*' and that for a negative sloped element in the same bay is '*5-x2-2*'. Similarly, in diagrid and framed tube systems, level-wise groups are created and elements are differentiated by 'closing' or 'opening' elements.

6.3 Material Properties and Loads

Materials

The steel columns, beams and bracings of the building are assumed to be of grade A992/A992M. The floor slabs, although not modelled, are assumed to be of high strength reinforced concrete. Table 6.3 summarizes the material properties.

Material	**Structural element**	**Material Property**	**Value**
Steel, Grade A992	Columns & Beams	Mass density	500 lb/ft^3
		Elastic Modulus	29,009,200 *psi*
		Yield stress	50 x 10^3 *psi*
		Poisson's ratio	0.3
Concrete	Floor slabs	Mass density	150 lb/ft^3
		Elastic Modulus	5.8 x 10^6 *psi*
		Yield stress	580.184 *psi*
		Poisson's ratio	0.15

Table 6.2 Material properties

Loads

The dead loads on the structure include self-weight of the concrete in floor slabs, self-weight of floor decks and floor finish loads. Assuming the building is for office use, the live loads are in accordance with the specifications provided in Table 4-1 of ASCE-7-10, '*Minimum Design Loads for Buildings and Other Structures*'. The table requires the loads to be a minimum of 50 *psf*. All the FE models have been designed for 70 *psf*. Wind loading is in accordance with the specifications provided in Chicago Building Code, Division 16, Table 13-52-310, Minimum Design Wind Pressures. For detailed interpolation and graphical representation of the said wind loads, please refer Appendix A. Following table shows the intensities of loading in a typical model.

Type	Description	Intensity
		psf
DL	Selfweight of concrete	48.30
	Selfweight of floor deck	4.10
	Floor finish	21.00
	Total (Dead)	73.40
LL	ASCE 7-10 - minimum 50 *psf*	70.00
	Total (Dead + live)	**143.40**

Table 6.3 Dead and live load intensities

Therefore, for a frame span '*S*' of 20 *ft*,

UDL intensity on all beams = 143.40 *psf*. x 20 *ft* / 12 *in*

= **239** *lb/in*

Load combinations

All models are designed for four static Allowable Stress Design (ASD) load combinations as specified in ASCE 7-10. Following are the load combinations.

1. LC 1 – Dead load + live load
2. LC 2 – Dead load + 0.6 wind load
3. LC 3 – Dead load + 0.75 live load + 0.75(0.6 wind load)
4. LC 4 – 0.6 Dead load + 0.6 wind load

All above load cases are also checked for buckling analysis as described in section 2.2. Along with above mentioned load cases, one load case of modal analysis is also being carried out.

For modal analysis, point masses are added for gravity loads (DL+LL) on every node. The intensity of the gravity loads from Table 6.3.2 is 143.4 *psf* ~1 psi. Therefore, the point mass on a particular node is the tributary area covered by that node. Now, since the tributary area is a function of the nodal coordinates, the point masses are defined as a

function of coordinates. Following table shows the point mass calculations. *'S'* is the span between frames (240") and X_1, X_2, X_3 and X_4 are nodal x coordinates at the right end of bay 1, bay 2, bay 3 and bay 4 respectively.

Node	Point mass
	lbm
1	S (X_1) / (2 x 386.4)
2	S (X_2) / (2 x 386.4)
3	S (X_3 - X_1) / (2 x 386.4)
4	S (X_4 - X_2) / (2 x 386.4)
5	S (X_3 - X_1) / (2 x 386.4)
6	S (X_2) / (2 x 386.4)
7	S (X_1) / (2 x 386.4)

Table 6.4 Point mass calculations

6.4 Numerical results

6.4.1 General model information

All structures are designed for AISC 2010 constraints as well as for fixed allowable stresses (strength based design). The general model and design related information is shown in the following table. As described in chapter 4, all frame models are designed to minimize the weight as the objective function.

Model	**Design Variables (CDV, DDV (Beam, Col., Bracing))**	**Number of Constra-ints**	**Best performing model**	**Pop. Size**	**Time for 100 FE (*s*)**
10F-Int-SBD	0, 17 (12, 5, 0)	2218	Sizing	170	1.8
20F-Int-SBD	2, 25 (15, 10, 0)	5819	Sizing + Shape	270	3.8
40F-Int-SBD	2, 62 (42, 20, 0)	8698	Sizing + Shape	640	7.6
60F-Int-SBD	0, 75 (45, 30, 0)	13016	Sizing + Shape	750	11.8
10F-Int-AISC	2, 17 (12, 5, 0)	4819	Sizing + Shape	190	2.1
20F-Int-AISC	2, 25 (15, 10, 0)	9579	Sizing + Shape	270	4.1
40F-Int-AISC	2, 62 (42, 20, 0)	19099	Sizing + Shape	640	8.6
60F-Int-AISC	2, 75 (45, 30, 0)	28618	Sizing + Shape	770	13.6
10F-Ext-SBD	2, 19 (12, 5, 2)	2266	Framed Tube	210	1.8
20F-Ext-SBD	0, 31 (15, 10, 6)	4811	Diagrid	310	3.9
40F-Ext-SBD	2, 70 (42, 20, 8)	8888	Framed Tube	720	8.0
60F-Ext-SBD	0, 95 (45, 30, 20)	14459	Diagrid	950	12.5
10F-Ext-AISC	2, 19 (12, 5, 2)	5459	Pyramid	210	2.3
20F-Ext-AISC	0, 31 (15, 10, 6)	10859	Pyramid	310	4.7
40F-Ext-AISC	2, 70 (42, 20, 8)	21659	Pyramid	720	9.6
60F-Ext-AISC	2, 105 (45, 30, 30)	32459	Diagrid	1070	15.9

Table 6.5 General design related information

The design variables are of two types, viz., CDV and DDV. The first number denotes the number of CDVs and second denoted DDVs. The parenthesis shows the breakdown of DDVs – number of beam DDVs, number of column DDVs and number of bracing DDVs.

Although, design process was carried out for all previously described exterior frames, results are being discussed only for the ‘best performing’ models. The performance is quantified solely based on the resultant weight of the frame. It is observed with AISC constraints that exterior frames with pyramid type of bracing system performs better than all up to 40F models. And with 60F model, diagrid resulted in lowest weight. This is necessarily due to shorter length of the bracing members as compared to diagrid and framed tube systems.

As it should be, the time required per function evaluation (FE) grows exponentially with a linear increase in building. The population size is 10 times the number of design variables.

6.4.2 Design properties

As seen in table 6.6, for most of the planar frames, LC3 – D + 0.75L + 0.45W is the controlling load case. Meaning, one of the variables is being utilized most in this particular load case. Although LC3 seems to be controlling, LC2 – D + 0.6L results in most of variables reaching high utilization as the story height increases and the wind load becomes dominant. Typically, wind load is observed to be rather dormant in 10F and 20F structures. This is due to low intensity of WL for lower heights. Please refer Appendix A for the overall intensities of wind loads according to Chicago Building Code. For these models, LC1 – D + L results in high utilization of most variables.

Model	Design Controlled By	Smallest Buckling Factor	Highest Period *(s)*	Max. Lateral Disp *(in)*
10F-Int-SBD	Comp. 1-C5 (D+0.75L +0.45W)	14.6	2.8	2.5
20F-Int-SBD	Tens. 9-B5 (D+0.75L +0.45W)	11.7	4.2	6.0
40F-Int-SBD	Disp. 41-1 (D+0.6W)	16.0	5.4	12.5
60F-Int-SBD	Comp. 15-C6 (D+0.75L +0.45W)	21.7	6.0	18.6
10F-Int-AISC	Comp. + Bend. 10-B1 (D+L)	15.4	2.6	2.1
20F-Int-AISC	Disp. 21-1 (D + 0.6W)	9.8	3.8	6.3
40F-Int-AISC	Comp. + Bend. 3-C4 (D+L)	14.5	5.4	12.1
60F-Int-AISC	Comp. + Bend. 29-C7 (D+0.75L +0.45W)	23.9	6.1	17.7
10F-Ext-SBD	Tens. 5-B5 (D+L)	28.0	1.4	0.7
20F-Ext-SBD	Comp. 5-C3 (D+L)	17.7	2.2	2.4
40F-Ext-SBD	Comp. 7XC2 (D+0.75L+0.45W)	23.7	4.5	8.5
60F-Ext-SBD	Comp. 7XO5 (D+0.75L+0.45W)	22.3	4.9	17.9
10F-Ext-AISC	Tens. + Bend. 7-B3 (D+L)	29.3	1.5	0.8
20F-Ext-AISC	Comp. + Bend. 7-C2 (D+L)	21.3	2.5	2.5
40F-Ext-AISC	Comp. + Bend. 14-C6 (D+0.75L+0.45W)	15.2	4.6	10.8
60F-Ext-AISC	Tens. + Bend. 45-B4 (D+L)	28.5	5.0	12.5

Table 6.6 Controlling factors and design properties

It is observed in the AISC models that columns are being utilized fully but beam elements are not. As seen in table 6.6, combined effect of compression and bending is the limit state for which, most of the models are designed. The primary function of the beam elements shifts from just carrying the loads to providing the complementary moment of inertia to provide rotational stiffness to the column elements, as the building height increases. This is necessarily to increase the degree of fixity for columns, which results in increased buckling strength and allows for the columns to be designed in the limit state of yielding. Unnecessary to mention, limit state of yielding results in higher load carrying capacity as compared to any other limit states in compression design (refer section 3.1.2).

As stated in section 3.1.2, the structure needs to designed in such a manner that the lowest Eigenvalue should be greater than 1 in order to bypass the limit state of flexural buckling. The buckling analyses carried out on the designed structures satisfy this criterion by a huge margin.

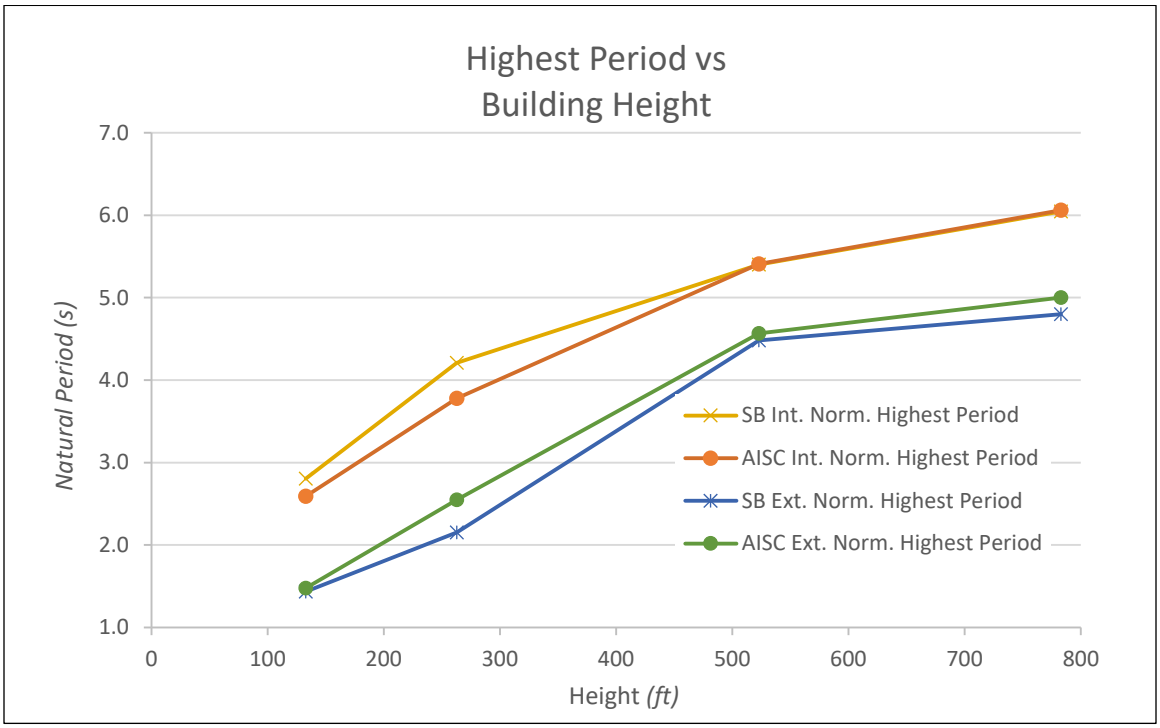

Figure 6.6 Highest period vs building height

In both, internal 'rigid' frames and external braced frames, it is observed that highest natural period of the frames appear to be converging. Bracing systems help to enhance the modal performance of the frames. Also, SB internal frames perform almost hand in hand with AISC internal frames. This is also true for external frames. The best performing model in the case if strength based external frames for 40F models is Framed Tube, whereas in the case of AISC based 40F, Pyramid type bracings perform better. As far as modal performance is concerned, Diagrid and Framed tube systems outperformed

any other type. On an average, Diagrid and Framed tube systems provide 30-40% lower highest periods as compared to the next best Pyramid systems.

6.4.3 Weight performance

In both internal and external models and in both SB and AISC based designs, beam weight contribution towards the entire structures weight gradually decreases as the height of the building increases. For 10F models, the beam weight contribution ranges from 40-50%, and that reduces to 12-20% in the case of 60F models.

In general, columns are designed heavier with the AISC constraints as compared to strength based models. This is due to allowable compressive stresses in SB designs are 30 ksi, and that with AISC constraints works out to be 22.5 ksi. It should be noted that this allowable value varies as a function of length of the member, section dimensions etc. in accordance with AISC limit states. As a result, the weight contribution of beams is lower in most cases of AISC based designs.

The normalized weight (weight per designed unit area) is computed by assuming a square building with 14 frames as

$$W_N = \frac{5W_{Int} + 5W_{Int,Beam} + 5\frac{2}{7}W_{Int,Col} + 4W_{Ext,Beam} + \frac{4}{7}W_{Ext,Col} + 4W_{Brac.}}{N_{Stories}(36S^2)} \tag{6.5}$$

Where, W_{Int} is the weight of the interior frame, W_{Ext} is the weight of the exterior frame and $N_{Stories}$ is the number of stories in the structure. It should be noted that the weight is calculated center-to-center without accounting for connections.

In the normalized weight calculations, only the weight of structural steel elements (beams, columns and bracing members) are included. Following table illustrate weight performance from the optimization results.

Model	**Beam weight *(ton)***	**Column weight *(ton)***	**Bracing weight *(ton)***	**Total weight *(ton)***	**Beam weight *(%)***	**Normalized weight *(psf)***
10F-Int-SBD	25.1	24.1	-	49.2	51.0	Calculated for combined internal + external frames
20F-Int-SBD	53.0	83.1	-	136.1	38.9	
40F-Int-SBD	176.5	355.3	-	531.8	33.2	
60F-Int-SBD	481.6	808.5	-	1290.1	37.3	
10F-Int-AISC	25.6	29.7	-	55.3	46.3	
20F-Int-AISC	59.2	97.5	-	156.7	37.8	
40F-Int-AISC	192.7	391.7	-	584.4	33.0	
60F-Int-AISC	459.1	884.5	-	1343.6	34.2	
10F-Ext-SBD	21.5	22.4	2.9	46.8	45.9	7.2
20F-Ext-SBD	48.5	68.9	14.4	134.6	36.0	9.4
40F-Ext-SBD	130.7	304.8	18.4	453.8	28.8	16.7
60F-Ext-SBD	196.7	749.4	94.1	1040.1	18.9	26.9
10F-Ext-AISC	20.1	27.9	2.6	50.6	39.7	7.7
20F-Ext-AISC	45.4	99.2	8	152.6	29.8	10.3
40F-Ext-AISC	128.3	347.1	23.1	498.4	25.7	18.2
60F-Ext-AISC	122.9	804.6	146	1073.4	11.4	27.3

Table 6.7 Weight performance from optimization results

As mentioned by Ali and Moon[5], there is a premium for height for taller structures due to lateral loads. As a result, total structural material consumption increases exponentially with a linear increase of height. This effect can be clearly seen from table 6.7 and figure 6.7.

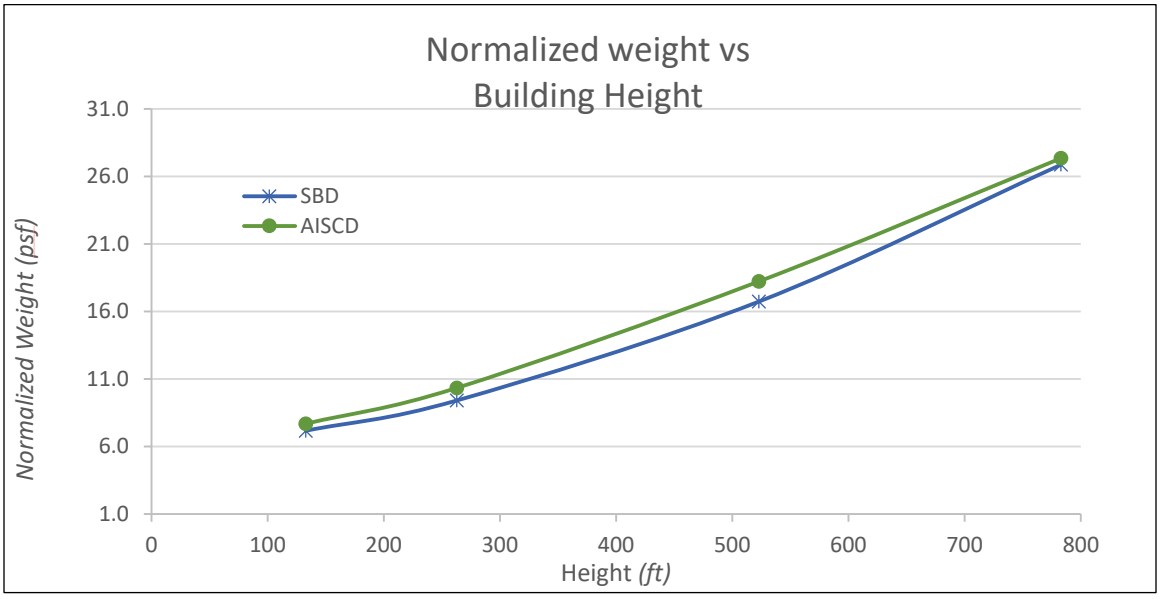

Figure 6.7 Normalized weight vs Building height

In figure 6.7, it can be seen that despite the fact that the bracing systems varies throughout the SB models, the plots for normalized weights of SB and AISC based models are parallel. The exponential nature of the plots can be clearly seen in these plots. As a general observation and according to the allowable stress value calculations, AISC based designs are, on an average, 7% heavier as compared to strength based designs.

A regression analysis was carried out on both the curves. Curve for models with strength based constraints follow the equation

$$N_{w\,[SB]} = 5.71\, e^{1.988E\text{-}03\,(Height)}$$

And curve for models with AISC constraints follow the equation

$$N_{w\,[AISC]} = 6.501\, e^{1.85E\text{-}03\,(Height)}$$

Where, N_w is in *psf* and Height is in *ft*.

7 CONCLUSIONS

This thesis presents a design methodology in accordance with AISC Steel Construction Manual 2010 Specifications. An algorithm has been developed for I-sections and implemented in GS-USA Frame3D program.

One of the most tedious tasks in these design checks is to compute the *'K'* factors for compression members in the limit state of flexural buckling. One of the provisions to bypass these calculations for every compression member in a finite element model is described in section E3 and Appendix 7, Section 7.2.3(b). This provision needs a satisfactory side-sway buckling analysis in order to bypass these calculations. This provision has been developed in the algorithm and implemented in Frame3D program.

This work also concentrates on structural design optimization of interior and exterior planar frames of ten, twenty, forty and sixty storey buildings. For exterior frames, six different types of bracing systems are designed and optimized for all four buildings. All models are optimized with AISC 2010 constraints as well as strength based constraints (as separate finite element models) for comparison purposes. Also, lateral deflection, inter-story drift and Euler buckling constraints are enforced in all models.

A database of 189 selective W shapes was extracted out of all 273 AISC standard sections. These sections have a higher moment of inertia to c/s area ratio as compared to the rest 84 discarded sections. In order to be able to use gradient-based optimization technique of MFD, a satisfactory regression analysis was performed to obtain the relationships between c/s area and general properties of the section. Following are the key features of the optimization results –

1. With AISC constraints, Pyramid bracing system outperforms all other bracing systems, as far as weight of the structure is concerned up to 40F. For 60F models, Diagrids performed better
2. With strength based constraints, best performing bracing system varies with the building height. Typically, framed tube and diagrid systems are observed to results in lowest structure weight.
3. Regardless of the type of constraint, type of bracing or height of the model, highest magnitude of lateral deflection is observed in the load case – Dead + 0.6 Wind.
4. It is observed that the wind load becomes dominant for structures higher than 40 stories since the intensity of the wind load increases exponentially.
5. All models designed have the lowest Buckling analysis Eigenvalue of greater than 1, which is required for aforementioned modified design procedure in section 3.1.2.
6. As far as modal analysis and wind resistance is concerned, Diagrid and framed tube systems perform better than any other bracing system. On an average, these systems result in 60-70% higher fundamental frequencies. Lateral displacements with these systems are about half of the 'best performing' pyramid systems. Vertical displacements are, on an average, 75% of the pyramid systems.
7. The bracing systems named Bay 1 & 6, 2 & 5 and 3 & 4 (figure 6.5) performed better than the rigid internal frames. The performance as compared to Pyramid, Diagrid and Framed tube systems was mediocre in regards to normalized weight,

lateral and vertical deflections, highest period and Buckling Eigenvalues for all the four exterior frame model heights.

8. It is observed that there is a gradual decrease in the beam weight contribution as the height of the structure increases. It drops from 40-50% in 10F models to around 12% in 60F models.
9. Columns in the models with AISC constraints require heavier sections as compared to strength based design models. Also, in almost all the models, the column elements have a higher utility ratio as compared to beam utility ratio.
10. The AISC constraint based models are designed 10% heavier (normalized steel consumption) on an average as compared to strength based models.
11. As established by Dr. Fazlur Khan, there exists a *'premium for height'*. The normalized structural steel consumption increases exponentially with a linear increase in height of the structure.

REFERENCES

[1] Victor E. Saouma, "lecture notes in structural engineering", University of Colorado, 2007.

[2] "ETABS receives 'Top Seismic Product of the 20th Century' Award", Press release. Structure magazine, 2006.

[3] Baker, William F., "Structural Innovation", Tall buildings and urban habitat: cities in the third millennium, New York: Spon Press. pp. 481–493. ISBN 0-415-23241-4, 2001.

[4] Bayley, Stephen, "Burj Dubai: The new pinnacle of vanity", Telegraph (London), 2010.

[5] Ali and Moon, "Structural developments in tall buildings: Current trends and future prospects", Architectural Science Review, Vol. 50.3, pp 205-223, 2007.

[6] S. D. Rajan, "Introduction to Structural Analysis and Design", Wiley, 2013.

[7] David S. Burnett, "Finite Element Analysis: From Concepts to Applications", Addison-Wesley, 1988.

[8] William McGuire, Richard H. Gallagher and Ronald D. Ziemian, "Matrix Structural Analysis, Second Edition", Section 12.8, pp 360.

[9] Jack C. McCormac, "Structural Steel Design, Second Edition", Section 18-9 Flexure-shear interaction, pp. 605.

[10] Kyoung Sun Moon, "Material-Saving Design Strategies for Tall Building Structures", CTBUH 2008 8th World Congress, Dubai, 2008.

[11] C. M. Chan, D. E. Grierson and N. Sherbourne, "Automatic Optimal Design of Tall Steel Building Frameworks".

APPENDIX A

DESIGN WIND LOADS DERIVED FROM CHICAGO BUILDING CODE, DIV. 16, TABLE 13-52-310

Storey	Height	Wind Pressure	
	(ft)	Nodal load *(psf)*	Nodal load *(lb)*
1	16	20.00	33.33
2	29	20.00	33.33
3	42	20.00	33.33
4	55	20.00	33.33
5	68	20.00	33.33
6	81	20.00	33.33
7	94	20.00	33.33
8	107	20.00	33.33
9	120	20.00	33.33
10	133	20.00	33.33
11	146	20.00	33.33
12	159	20.00	33.33
13	172	20.00	33.33
14	185	20.00	33.33
15	198	20.00	33.33
16	211	20.11	33.52
17	224	20.24	33.73
18	237	20.37	33.95
19	250	20.50	34.17
20	263	20.63	34.38
21	276	20.76	34.60
22	289	20.89	34.82
23	302	21.08	35.13
24	315	21.60	36.00
25	328	22.12	36.87
26	341	22.64	37.73
27	354	23.16	38.60
28	367	23.68	39.47
29	380	24.20	40.33
30	393	24.72	41.20

Storey	Height	Wind Pressure	
	(ft)	Nodal load *(psf)*	Nodal load *(lb)*
31	406	25.18	41.97
32	419	25.57	42.62
33	432	25.96	43.27
34	445	26.35	43.92
35	458	26.74	44.57
36	471	27.13	45.22
37	484	27.52	45.87
38	497	27.91	46.52
39	510	28.30	47.17
40	523	28.69	47.82
41	536	29.08	48.47
42	549	29.47	49.12
43	562	29.86	49.77
44	575	30.25	50.42
45	588	30.64	51.07
46	601	31.02	51.70
47	614	31.28	52.13
48	627	31.54	52.57
49	640	31.80	53.00
50	653	32.06	53.43
51	666	32.32	53.87
52	679	32.58	54.30
53	692	32.84	54.73
54	705	33.15	55.25
55	718	33.54	55.90
56	731	33.93	56.55
57	744	34.32	57.20
58	757	34.71	57.85
59	770	35.10	58.50
60	783	35.49	59.15

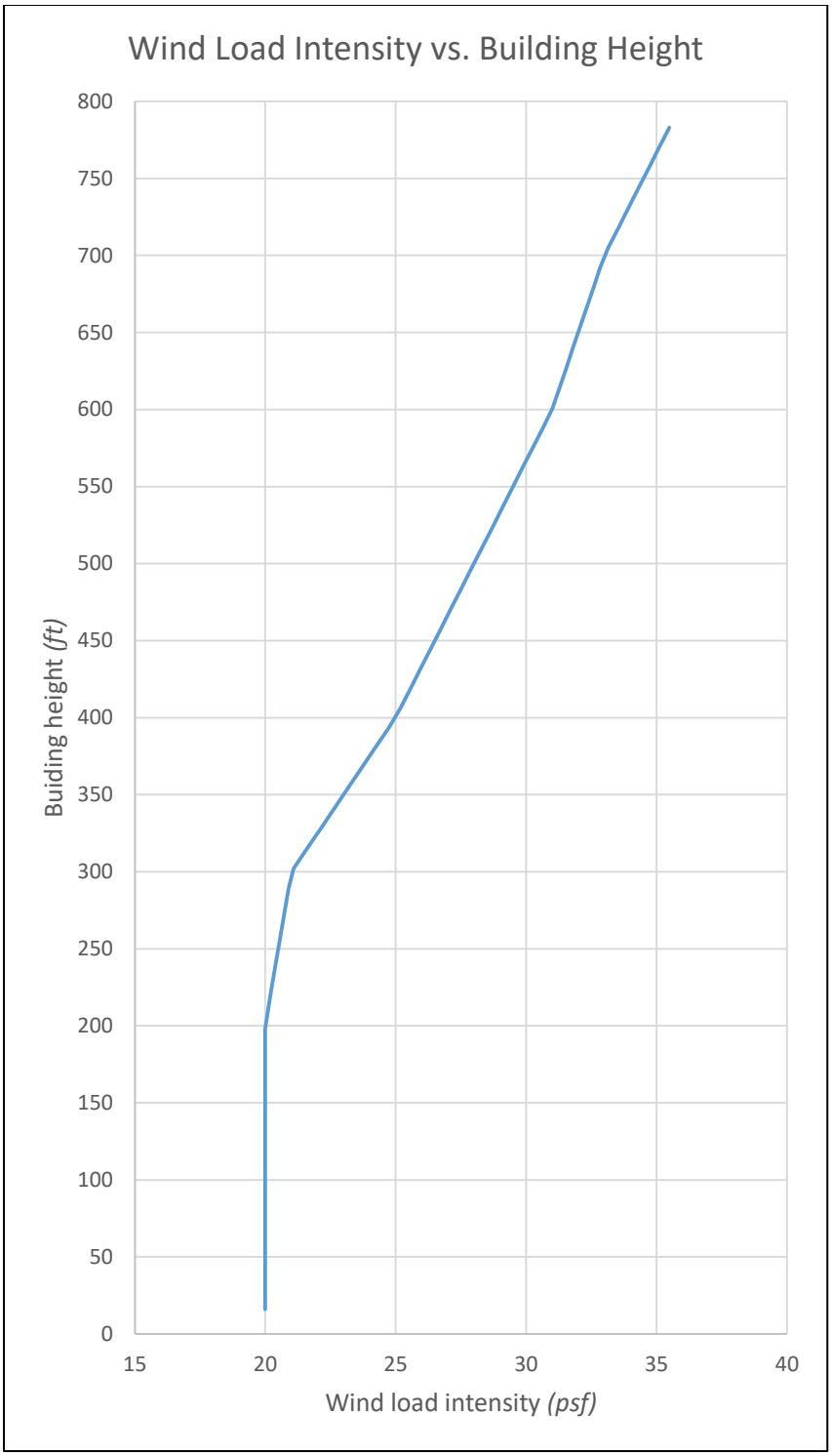
Wind Load Intensity vs. Building Height
Buiding height (ft)
800
750
700
650
600
550
500
450
400
350
300
250
200
150
100
50
0
15
20
25
30
35
40
Wind load intensity (psf)

APPENDIX B

AISC WIDE FLANGE SECTIONS SELECTED IN THE DDV TABLE

Symbol	Property description
Line	Line number in the DDV table
Property	Cross section tag for wide flange section
Area	Cross sectional area
Iz	Moment of inertia about local *z* axis
Iy	Moment of inertia about *y* axis
J	Torsional constant 0.833*Cross sectional area
Sz	Section modulus about the local *z* axis
Sy	Section modulus about the local *y* axis
SFz	"Shear factor" for computing shear stress (shear force acting in the local z direction)
SFy	"Shear factor" for computing shear stress (shear force acting in the local *y* direction)
TF	"Torsional factor" for computing the shear stress due to torsional moment

Line	Property	Area	Iz	Iy	J	Sz	Sy	SFz	SFy	TF
1	WF 6x8.5	2.52	14.9	1.99	0.03	5.1	1.01	0.5	0.91	0.15
2	WF 6x9	2.68	16.4	2.2	0.04	5.56	1.11	0.55	0.92	0.18
3	WF 8x10	2.96	30.8	2.09	0.04	7.81	1.06	0.52	1.22	0.18
4	WF 10x12	3.54	53.8	2.18	0.05	10.9	1.1	0.53	1.67	0.23
5	WF 6x12	3.55	22.1	2.99	0.09	7.31	1.5	0.72	1.25	0.31
6	WF 4x13	3.83	11.3	3.86	0.15	5.46	1.9	0.91	1.02	0.42
7	WF 8x13	3.84	39.6	2.73	0.09	9.91	1.37	0.65	1.64	0.31
8	WF 12x14	4.16	88.6	2.36	0.07	14.9	1.19	0.56	2.09	0.29
9	WF 10x15	4.41	68.9	2.89	0.1	13.8	1.45	0.68	2.03	0.37
10	WF 6x15	4.43	29.1	9.32	0.1	9.72	3.11	1.02	1.26	0.37
11	WF 8x15	4.44	48	3.41	0.14	11.8	1.7	0.81	1.77	0.42
12	WF 5x16	4.71	21.4	7.51	0.19	8.55	3	1.19	1.08	0.52
13	WF 12x16	4.71	103	2.82	0.1	17.1	1.41	0.66	2.31	0.38
14	WF 6x16	4.74	32.1	4.43	0.22	10.2	2.2	1.06	1.45	0.57
15	WF 10x17	4.99	81.9	3.56	0.16	16.2	1.78	0.84	2.15	0.48
16	WF 8x18	5.26	61.9	7.97	0.17	15.2	3.04	1.13	1.7	0.52
17	WF 12x19	5.57	130	3.76	0.18	21.3	1.88	0.89	2.5	0.55
18	WF 10x19	5.62	96.3	4.29	0.23	18.8	2.14	1.02	2.28	0.62
19	WF 8x21	6.16	75.3	9.77	0.28	18.2	3.71	1.38	1.87	0.73
20	WF 12x22	6.48	156	4.66	0.29	25.4	2.31	1.09	2.81	0.75
21	WF 10x22	6.49	118	11.4	0.24	23.2	3.97	1.35	2.2	0.69
22	WF 14x22	6.49	199	7	0.21	29	2.8	1.08	2.85	0.61
23	WF 10x26	7.61	144	14.1	0.4	27.9	4.89	1.66	2.43	0.97
24	WF 12x26	7.65	204	17.3	0.3	33.4	5.34	1.61	2.56	0.83
25	WF 16x26	7.68	301	9.59	0.26	38.4	3.49	1.21	3.48	0.76
26	WF 14x26	7.69	245	8.91	0.36	35.3	3.55	1.35	3.18	0.88
27	WF 12x30	8.79	238	20.3	0.46	38.6	6.24	1.87	2.91	1.11
28	WF 10x30	8.84	170	16.7	0.62	32.4	5.75	1.93	2.81	1.31
29	WF 14x30	8.85	291	19.6	0.38	42	5.82	1.69	3.4	0.99

Line	Property	Area	Iz	Iy	J	Sz	Sy	SFz	SFy	TF
30	WF 16x31	9.13	375	12.4	0.46	47.2	4.49	1.56	3.88	1.1
31	WF 10x33	9.71	171	36.6	0.58	35	9.2	2.28	2.62	1.26
32	WF 14x34	10	340	23.3	0.57	48.6	6.91	1.99	3.6	1.3
33	WF 12x35	10.3	285	24.5	0.74	45.6	7.47	2.23	3.37	1.54
34	WF 18x35	10.3	510	15.3	0.51	57.6	5.12	1.62	4.68	1.24
35	WF 16x36	10.6	448	24.5	0.55	56.5	7	1.95	4.18	1.31
36	WF 14x38	11.2	385	26.7	0.8	54.6	7.88	2.27	3.94	1.63
37	WF 10x39	11.5	209	45	0.98	42.1	11.3	2.78	2.87	1.81
38	WF 12x40	11.7	307	44.1	0.91	51.5	11	2.71	3.25	1.75
39	WF 16x40	11.8	518	28.9	0.79	64.7	8.25	2.29	4.39	1.67
40	WF 18x40	11.8	612	19.1	0.81	68.4	6.35	2.02	4.99	1.68
41	WF 14x43	12.6	428	45.2	1.05	62.6	11.3	2.78	3.84	1.91
42	WF 21x44	13	843	20.7	0.77	81.6	6.37	1.84	6.31	1.7
43	WF 12x45	13.1	348	50	1.26	57.7	12.4	3.04	3.68	2.21
44	WF 10x45	13.3	248	53.4	1.51	49.1	13.3	3.28	3.21	2.44
45	WF 16x45	13.3	586	32.8	1.11	72.7	9.34	2.57	4.98	2.11
46	WF 18x46	13.5	712	22.5	1.22	78.8	7.43	2.34	5.71	2.23
47	WF 14x48	14.1	484	51.4	1.45	70.2	12.8	3.13	4.3	2.4
48	WF 21x48	14.1	959	38.7	0.8	93	9.52	2.24	6.41	1.83
49	WF 10x49	14.4	272	93.4	1.39	54.6	18.7	3.7	3.11	2.45
50	WF 12x50	14.6	391	56.3	1.71	64.2	13.9	3.39	4.09	2.73
51	WF 16x50	14.7	659	37.2	1.52	81	10.5	2.88	5.49	2.62
52	WF 18x50	14.7	800	40.1	1.24	88.9	10.7	2.76	5.69	2.36
53	WF 21x50	14.7	984	24.9	1.14	94.5	7.64	2.2	6.94	2.22
54	WF 12x53	15.6	425	95.8	1.58	70.6	19.2	3.79	3.83	2.66
55	WF 14x53	15.6	541	57.7	1.94	77.8	14.3	3.48	4.71	2.94
56	WF 10x54	15.8	303	103	1.82	60	20.6	4.08	3.42	2.95
57	WF 18x55	16.2	890	44.9	1.66	98.3	11.9	3.06	6.28	2.88
58	WF 21x55	16.2	1140	48.4	1.24	110	11.8	2.76	6.92	2.44
59	WF 24x55	16.2	1350	29.1	1.18	114	8.3	2.21	8.07	2.39
60	WF 21x57	16.7	1170	30.6	1.77	111	9.35	2.69	7.47	2.97
61	WF 16x57	16.8	758	43.1	2.22	92.2	12.1	3.28	6.27	3.39
62	WF 12x58	17	475	107	2.1	78	21.4	4.23	4.04	3.23
63	WF 18x60	17.6	984	50.1	2.17	108	13.3	3.38	6.73	3.44
64	WF 10x60	17.7	341	116	2.48	66.7	23	4.5	3.89	3.67
65	WF 14x61	17.9	640	107	2.19	92.1	21.5	4.22	4.78	3.39
66	WF 24x62	18.2	1550	34.5	1.71	131	9.8	2.6	8.86	3.06
67	WF 21x62	18.3	1330	57.5	1.83	127	14	3.26	7.47	3.16
68	WF 12x65	19.1	533	174	2.18	87.9	29.1	4.79	4.38	3.51
69	WF 18x65	19.1	1070	54.8	2.73	117	14.4	3.66	7.26	4.04
70	WF 16x67	19.6	954	119	2.39	117	23.2	4.5	5.88	3.82
71	WF 10x68	19.9	394	134	3.56	75.7	26.4	5.19	4.4	4.7
72	WF 14x68	20	722	121	3.01	103	24.2	4.77	5.35	4.22
73	WF 21x68	20	1480	64.7	2.45	140	15.7	3.64	8.08	3.85
74	WF 24x68	20.1	1830	70.4	1.87	154	15.7	3.36	8.73	3.37
75	WF 18x71	20.9	1170	60.3	3.49	127	15.8	3.96	8	4.79
76	WF 12x72	21.1	597	195	2.93	97.4	32.4	5.36	4.82	4.31

Line	Property	Area	Iz	Iy	J	Sz	Sy	SFz	SFy	TF
77	WF 21x73	21.5	1600	70.6	3.02	151	17	3.94	8.57	4.44
78	WF 14x74	21.8	795	134	3.87	112	26.6	5.17	5.76	5.05
79	WF 18x76	22.3	1330	152	2.83	146	27.6	4.93	7.01	4.45
80	WF 24x76	22.4	2100	82.5	2.68	176	18.4	3.93	9.34	4.27
81	WF 16x77	22.6	1110	138	3.57	134	26.9	5.1	6.79	5.05
82	WF 10x77	22.7	455	154	5.11	85.9	30.1	5.84	4.99	6.06
83	WF 12x79	23.2	662	216	3.84	107	35.8	5.84	5.28	5.22
84	WF 14x82	24	881	148	5.07	123	29.3	5.7	6.59	6.09
85	WF 21x83	24.4	1830	81.4	4.34	171	19.5	4.46	9.73	5.7
86	WF 24x84	24.7	2370	94.4	3.7	196	20.9	4.46	10.04	5.28
87	WF 27x84	24.7	2850	106	2.81	213	21.2	4.07	10.88	4.57
88	WF 18x86	25.3	1530	175	4.1	166	31.6	5.57	7.95	5.74
89	WF 12x87	25.6	740	241	5.1	118	39.7	6.51	5.87	6.33
90	WF 16x89	26.2	1300	163	5.45	155	31.4	5.9	7.82	6.77
91	WF 30x90	26.3	3610	115	2.84	245	22.1	4.06	12.24	4.71
92	WF 14x90	26.5	999	362	4.06	143	49.9	6.83	5.7	5.73
93	WF 21x93	27.3	2070	92.9	6.03	192	22.1	4.99	11	7.17
94	WF 27x94	27.6	3270	124	4.03	243	24.8	4.76	11.7	5.79
95	WF 24x94	27.7	2700	109	5.26	222	24	5.09	11.06	6.7
96	WF 18x97	28.5	1750	201	5.86	188	36.1	6.38	8.95	7.29
97	WF 30x99	29	3990	128	3.77	269	24.5	4.41	13.44	5.76
98	WF 16x100	29.4	1490	186	7.73	175	35.7	6.72	8.84	8.55
99	WF 21x101	29.8	2420	248	5.21	227	40.3	6.43	9.61	6.96
100	WF 27x102	30	3620	139	5.28	267	27.8	5.34	12.37	6.92
101	WF 24x103	30.3	3000	119	7.07	245	26.5	5.63	11.9	8.13
102	WF 24x104	30.7	3100	259	4.72	258	40.7	6.18	10.76	6.75
103	WF 18x106	31.1	1910	220	7.48	204	39.4	6.85	9.85	8.66
104	WF 30x108	31.7	4470	146	4.99	299	27.9	5.04	14.3	6.92
105	WF 21x111	32.6	2670	274	6.83	249	44.5	7.08	10.66	8.36
106	WF 27x114	33.6	4080	159	7.33	299	31.5	5.97	13.68	8.68
107	WF 30x116	34.2	4930	164	6.43	329	31.3	5.68	14.92	8.16
108	WF 24x117	34.4	3540	297	6.72	291	46.5	7.08	11.97	8.53
109	WF 33x118	34.7	5900	187	5.3	359	32.6	5.39	15.85	7.44
110	WF 18x119	35.1	2190	253	10.6	231	44.9	7.72	10.97	11.03
111	WF 21x122	35.9	2960	305	8.98	273	49.2	7.75	11.62	10.11
112	WF 30x124	36.5	5360	181	7.99	355	34.4	6.27	15.55	9.39
113	WF 27x129	37.8	4760	184	11.1	345	36.8	7.06	14.89	11.35
114	WF 18x130	38.3	2460	278	14.5	256	49.9	8.65	11.32	13.46
115	WF 33x130	38.3	6710	218	7.37	406	37.9	6.3	16.92	9.22
116	WF 24x131	38.6	4020	340	9.5	329	53	7.97	13.2	10.8
117	WF 21x132	38.8	3220	333	11.3	295	53.5	8.44	12.65	11.86
118	WF 30x132	38.8	5770	196	9.72	380	37.2	6.78	16.47	10.69
119	WF 36x135	39.9	7800	225	7	439	37.7	5.93	18.59	9.17
120	WF 33x141	41.5	7450	246	9.7	448	42.7	7.12	17.82	11.01
121	WF 24x146	43	4580	391	13.4	371	60.5	9.16	14.37	13.54
122	WF 21x147	43.2	3630	376	15.4	329	60.1	9.36	14.06	14.64
123	WF 27x146	43.2	5660	443	11.3	414	63.5	8.83	14.93	12.1

Line	Property	Area	Iz	Iy	J	Sz	Sy	SFz	SFy	TF
124	WF 30x148	43.6	6680	227	14.5	436	43.3	7.87	17.5	13.9
125	WF 40x149	43.8	9800	229	9.36	513	38.8	6.19	21.43	10.36
126	WF 36x150	44.3	9040	270	10.1	504	45.1	7.15	19.65	11.62
127	WF 33x152	44.9	8160	273	12.4	487	47.2	7.77	18.67	13.05
128	WF 36x160	47	9760	295	12.4	542	49.1	7.81	20.61	13.25
129	WF 27x161	47.6	6310	497	15.1	458	70.9	9.88	16.4	14.74
130	WF 24x162	47.8	5170	443	18.5	414	68.4	10.21	15.61	16.84
131	WF 40x167	49.3	11600	283	14	600	47.9	7.71	22.39	13.64
132	WF 33x169	49.5	9290	310	17.7	549	53.9	8.98	20.02	16.29
133	WF 36x170	50	10500	320	15.1	581	53.2	8.47	21.64	15.09
134	WF 30x173	50.9	8230	598	15.6	541	79.8	10.37	17.92	15.64
135	WF 24x176	51.7	5680	479	23.9	450	74.3	11.2	16.79	19.92
136	WF 27x178	52.5	7020	555	20.1	505	78.8	10.86	18.06	17.97
137	WF 40x183	53.3	13200	331	19.3	675	56	9.09	22.79	16.65
138	WF 36x182	53.6	11300	347	18.5	623	57.6	9.01	23.07	17.39
139	WF 30x191	56.1	9200	673	21	600	89.5	11.65	19.52	19.12
140	WF 36x194	57	12100	375	22.2	664	61.9	9.72	24.42	19.68
141	WF 27x194	57.1	7860	619	27.1	559	88.1	12.3	18.92	21.78
142	WF 40x199	58.8	14900	695	18.3	770	88.2	10.82	22.7	17.36
143	WF 33x201	59.1	11600	749	20.8	686	95.2	11.82	21.71	19.39
144	WF 36x210	61.9	13200	411	28	719	67.5	10.44	26.53	23.16
145	WF 40x211	62.1	15500	390	30.4	786	66.1	10.65	26.21	22.98
146	WF 30x211	62.3	10300	757	28.4	665	100	12.92	21.45	23.46
147	WF 40x215	63.5	16700	803	24.8	859	101	12.55	22.96	21
148	WF 33x221	65.3	12900	840	27.8	759	106	13.07	23.52	23.79
149	WF 44x230	67.8	20800	796	24.9	971	101	12.34	27	22.68
150	WF 36x232	68	15000	468	39.6	809	77.2	12.11	28.19	28.85
151	WF 36x231	68.2	15600	940	28.7	854	114	13.43	24.91	24.25
152	WF 40x235	69.1	17400	444	41.3	875	74.6	11.87	29.06	28.56
153	WF 33x241	71.1	14200	933	36.2	831	118	14.32	25.22	28.31
154	WF 36x247	72.5	16700	1010	34.7	913	123	14.41	26.23	27.59
155	WF 40x249	73.5	19600	926	38.1	993	118	14.42	26.66	28.36
156	WF 36x256	75.3	16800	528	52.9	895	86.5	13.38	31.34	35.3
157	WF 36x262	77.2	17900	1090	41.6	972	132	15.36	27.57	31.29
158	WF 44x262	77.2	24100	923	37.3	1110	117	14.29	30.01	29.84
159	WF 33x263	77.4	15900	1040	48.7	919	131	16.17	26.84	34.27
160	WF 40x264	77.4	19400	493	56.1	971	82.6	13.03	33.61	35.5
161	WF 40x277	81.5	21900	1040	51.5	1100	132	16.15	29.59	35.05
162	WF 40x278	82.3	20500	521	65	1020	87.1	13.47	35.84	39.78
163	WF 36x282	82.9	19600	1200	52.7	1050	144	16.9	29.37	36.55
164	WF 44x290	85.4	27000	1040	50.9	1240	132	16.05	33.3	36.78
165	WF 33x291	85.6	17700	1160	65.1	1020	146	17.77	29.67	41.88
166	WF 40x294	86.2	21900	562	76.6	1080	93.5	14.54	37.3	44.21
167	WF 40x297	87.3	23200	1090	61.2	1170	138	16.82	33.08	39.68
168	WF 36x302	89	21100	1300	64.3	1130	156	18.06	31.36	42.03
169	WF 33x318	93.7	19500	1290	84.4	1110	161	19.47	32.09	50.11
170	WF 40x324	95.3	25600	1220	79.4	1280	153	18.56	35.57	47.52

Line	Property	Area	Iz	Iy	J	Sz	Sy	SFz	SFy	TF
171	WF 40x327	95.9	24500	640	103	1200	105	16.17	41.58	54.55
172	WF 36x330	96.9	23300	1420	84.3	1240	171	19.92	34.06	50.31
173	WF 40x331	97.7	24700	644	105	1210	106	15.94	42.68	56.09
174	WF 44x335	98.5	31100	1200	74.7	1410	150	18.12	39.79	48.14
175	WF 33x354	104	22000	1460	115	1240	181	21.68	36.1	61.91
176	WF 36x361	106	25700	1570	109	1350	188	21.69	37.59	60.03
177	WF 40x362	106	28900	1380	109	1420	173	20.64	40.07	59.23
178	WF 40x372	110	29600	1420	116	1460	177	20.94	41.4	62.4
179	WF 33x387	114	24300	1620	148	1350	200	23.7	39.33	73.99
180	WF 36x395	116	28500	1750	142	1490	208	23.83	41.13	72.17
181	WF 40x392	116	29900	803	172	1440	130	19.08	50.08	78.76
182	WF 40x397	117	32000	1540	142	1560	191	22.68	43.79	71.2
183	WF 40x431	127	34800	1690	177	1690	208	24.46	48.15	83.46
184	WF 36x441	130	32100	1990	194	1650	235	26.37	45.81	89.95
185	WF 36x487	143	36000	2250	258	1830	263	29.35	51.18	109.34
186	WF 40x503	148	41600	2040	277	1980	249	28.66	55.81	114.39
187	WF 36x529	156	39600	2490	327	1990	289	32.03	55.17	128.98
188	WF 40x593	174	50400	2520	445	2340	302	33.94	65.79	158.63
189	WF 36x652	192	50600	3230	593	2460	367	39.34	68.51	195.63

APPENDIX C

COLUMN MOMENT OF INERTIA REQUIREMENTS FOR BEST PERFORMING EXTERIOR STRUCTURES

Column	SBD	AISCD
	Braced Tube	Pyramid
	I_{zz} (in^4)	I_{zz} (in^4)
C 9-10	32.1	204
C 7-8	375	385
C 5-6	586	425
C 3-4	228	1170
C 1-2	1830	1530

Column	SBD	AISCD
	Diagrid	Pyramid
	I_{zz} (in^4)	I_{zz} (in^4)
C 19-20	61.9	144
C 17-18	375	428
C 15-16	248	341
C 13-14	1140	1330
C 11-12	795	1300
C 9-10	2370	4470
C 7-8	740	2960
C 5-6	2070	7450
C 3-4	2420	5170
C 1-2	4080	7020

Column	SBD	AISCD
	Braced Tube	Pyramid
	I_{zz} (in^4)	I_{zz} (in^4)
C 39-40	659	428
C 37-38	712	954
C 35-36	1480	541
C 33-34	1070	1170
C 31-32	2070	1300
C 29-30	2850	4080
C 27-28	1240	5360
C 25-26	2670	5770
C 23-24	4080	3630
C 21-22	7800	5170
C 19-20	2140	13200
C 17-18	11700	13200
C 15-16	1650	20800
C 13-14	17400	15600
C 11-12	4900	16700
C 9-10	19600	17900
C 7-8	9600	20500
C 5-6	15000	23200
C 3-4	5510	19500
C 1-2	16800	22000

Column	SBD	AISCD
	Diagrid	Diagrid
	I_{zz} (in^4)	I_{zz} (in^4)
C 59-60	307	156
C 57-58	1070	238
C 55-56	2850	959
C 53-54	2070	890
C 51-52	1490	1110
C 49-50	2670	2070
C 47-48	1430	3000
C 45-46	5770	5900
C 43-44	16700	10500
C 41-42	11700	8160
C 39-40	15500	7020
C 37-38	13200	20800
C 35-36	10800	13200
C 33-34	16700	16700
C 31-32	19400	21900
C 29-30	19600	21900
C 27-28	16200	21900
C 25-26	13100	19500
C 23-24	4060	25600
C 21-22	29900	22000
C 19-20	28900	32000
C 17-18	16200	24300
C 15-16	14600	32000
C 13-14	6000	41600
C 11-12	24500	32100
C 9-10	16200	36000
C 7-8	6600	50400
C 5-6	6000	41600
C 3-4	32000	39600
C 1-2	36000	50600